

1-1-1976

A computational study of a nine-point numerical approximation to the two-dimensional Poisson equation

Eugene Francis Eckholt
Iowa State University

Follow this and additional works at: <https://lib.dr.iastate.edu/rtd>



Part of the [Engineering Commons](#)

Recommended Citation

Eckholt, Eugene Francis, "A computational study of a nine-point numerical approximation to the two-dimensional Poisson equation" (1976). *Retrospective Theses and Dissertations*. 18379.
<https://lib.dr.iastate.edu/rtd/18379>

This Thesis is brought to you for free and open access by the Iowa State University Capstones, Theses and Dissertations at Iowa State University Digital Repository. It has been accepted for inclusion in Retrospective Theses and Dissertations by an authorized administrator of Iowa State University Digital Repository. For more information, please contact digirep@iastate.edu.

A computational study of a nine-point numerical approximation
to the two-dimensional Poisson equation

by

Eugene Francis Eckholt

A Thesis Submitted to the
Graduate Faculty in Partial Fulfillment of
The Requirements for the Degree of
MASTER OF SCIENCE

Department: Chemical Engineering and Nuclear Engineering
Major: Nuclear Engineering

Signatures have been redacted for privacy

Iowa State University
Ames, Iowa

1976

TABLE OF CONTENTS

	<u>Page</u>
CHAPTER 1. INTRODUCTION AND LITERATURE REVIEW	1
CHAPTER 2. THEORETICAL DEVELOPMENTS	7
CHAPTER 3. COMPUTATIONAL PROCEDURES	14
3.1 Analytical Solutions	14
3.2 Definitions of Error	19
3.3 Speed of Convergence and SOR Optimization	20
3.4 Description of Boundary Conditions	24
3.5 Description of Computer Program Used for Study	25
CHAPTER 4. RESULTS AND DISCUSSION	28
4.1 Introduction	28
4.2 Error Analysis Results	28
4.3 Convergence Analysis	51
4.4 Optimization of the SOR Technique	61
CHAPTER 5. CONCLUSIONS	66
CHAPTER 6. SUGGESTIONS FOR FURTHER STUDY	68
LITERATURE CITED	70
ACKNOWLEDGMENTS	71
APPENDIX A. DERIVATION OF FIVE-POINT FINITE DIFFERENCE APPROXIMATION TO THE TWO-DIMENSIONAL POISSON EQUATION	72
APPENDIX B. FLOW CHART OF COMPUTER PROGRAM USED BY THIS STUDY	75

CHAPTER 1. INTRODUCTION AND LITERATURE REVIEW

The mathematical formulation of most problems in science involving rates of change with respect to two or more variables leads either to a partial differential equation, or to a set of such equations. Special cases of the two-dimensional second order equation

$$a \frac{\partial^2 \phi}{\partial x^2} + b \frac{\partial^2 \phi}{\partial x \partial y} + c \frac{\partial^2 \phi}{\partial y^2} + f(x, y, \phi, \frac{\partial \phi}{\partial x}, \frac{\partial \phi}{\partial y}) = 0 \quad (1.1)$$

where a , b , and c may be functions of the independent variables x and y or of the dependent variable ϕ occur frequently. Equation 1.1 is classified as elliptic over a region if $b^2 - 4ac < 0$ at all points in the region. Two of the best known of the two-dimensional elliptic equations are Laplace's equation

$$\frac{\partial^2 \phi}{\partial x^2} + \frac{\partial^2 \phi}{\partial y^2} = 0 \quad (1.2)$$

and Poisson's equation

$$\frac{\partial^2 \phi}{\partial x^2} + \frac{\partial^2 \phi}{\partial y^2} + f(x, y) = 0 \quad (1.3)$$

which are generally associated with equilibrium or steady-state problems.

The analytical solution of a two-dimensional elliptic equation is a function $\phi(x, y)$, which satisfies the partial differential equation at every point in a region R , and satisfies certain boundary conditions on the closed curve surrounding R . The boundary conditions for an elliptic equation are made up of either the function ϕ , its normal derivative, or a linear combination of ϕ and the normal derivative.

However, only a limited number of special types of elliptic equations have been solved analytically, and their usefulness is limited even further to problems involving shapes for which the boundary conditions can be met. This not only eliminates all problems with boundaries that are undefined in terms of equations, but also many for which the boundary conditions are too difficult to satisfy even though the boundaries are defined in terms of equations. In such cases approximation methods, usually numerical in character, are the only means of solution. Of the numerical approximation methods available for solving differential equations, those employing finite differences are more frequently used than any other.

In the finite difference approach, the technique is to superimpose a rectangular grid over the region in question, see Fig. 1. The linear partial differential equation is then replaced by an algebraic system of simultaneous linear difference equations, one difference equation for each internal nodal point of the grid. This system can then, in turn, be solved by either direct or iterative techniques for the value of $\phi_{i,j}$ at each of the nodal points. As the grid spacing is reduced and therefore the number of nodal points increased, and if the solution converges, the values of $\phi_{i,j}$ should approach the analytical solution of the partial differential equation over the region.

The finite difference equations can be obtained using a Taylor's expansion method. The most widely applied finite difference equation is the five-point equation, such as that developed in Appendix A for

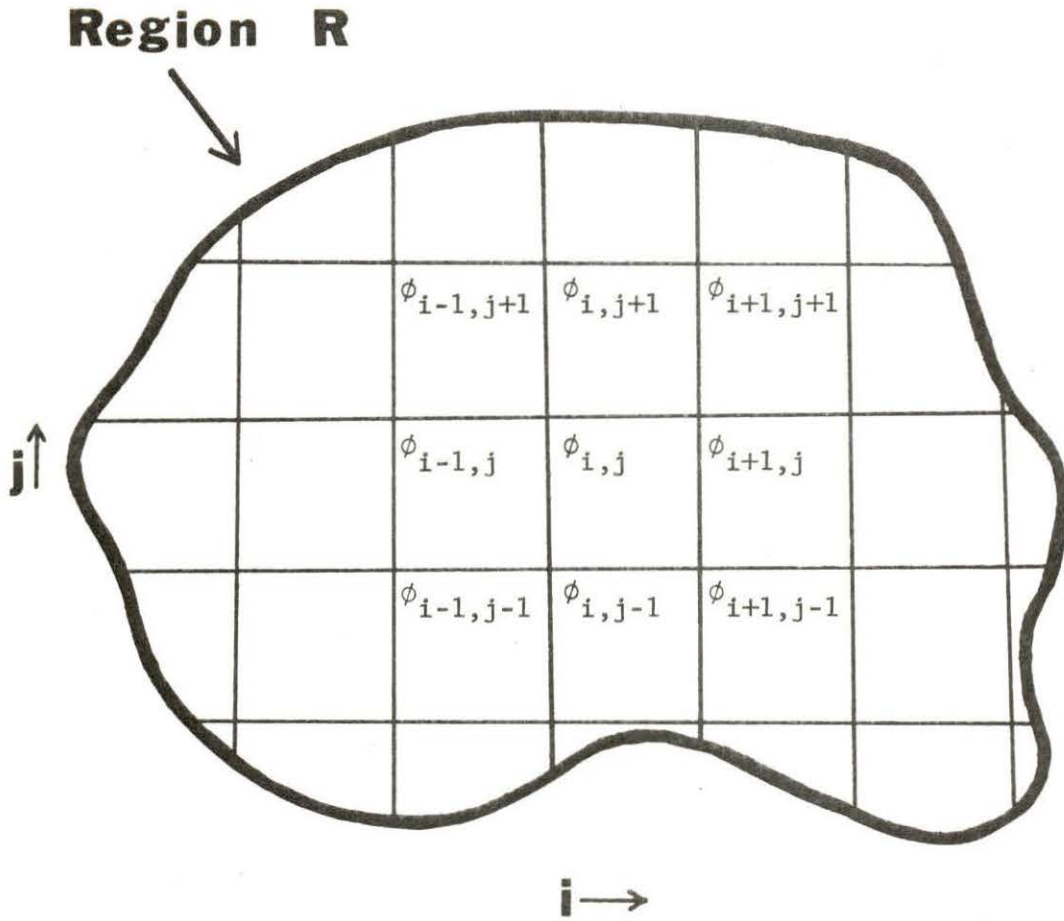


Fig. 1. General region R with rectangular grid for finite difference application.

Poisson's equation in two dimensions. Applied to Laplace's equation ($f(x, y) = 0$) the five-point difference equation from Appendix A is

(A-11)
$$\phi_{i,j} = \frac{r}{2(1+r^2)} \left[\frac{1}{r} (\phi_{i+1,j} + \phi_{i-1,j}) + r(\phi_{i,j+1} + \phi_{i,j-1}) \right] - h_1 h_2 (b_{ij}) - O(h^2) \quad (1.4)$$

where

$$r = \frac{h_1}{h_2}$$

Accuracy of the finite difference technique can be improved by representing the partial differential equation by a higher order finite difference approximation developed to reduce the truncation error. This is accomplished by using Taylor's expansions about the four corner points as well as the five previously expanded points. The resulting equation is a nine-point finite difference equation. A number of such formulae for the Laplacian operator and equal grid spacing have been developed [1, 2, 3, 4, 5, 6]. In general they take the form

$$\nabla^2 \phi_{i,j} = \frac{1}{6h^2} [4S_1 + S_2 - 20 \phi_{i,j}] - \frac{1}{12} h^2 \nabla^4 \phi_{i,j} + O(h^4) \quad (1.5)$$

where

$$S_1 = \phi_{i+1,j} + \phi_{i-1,j} + \phi_{i,j-1} + \phi_{i,j+1}$$

$$S_2 = \phi_{i+1,j+1} + \phi_{i-1,j+1} + \phi_{i+1,j-1} + \phi_{i-1,j-1}$$

and

$$\nabla^2 \phi_{i,j} = \nabla^2 \phi(x, y) \Big|_{\substack{x=x_i \\ y=y_j}}$$

Equation 1.5 can be applied to Laplace's equation by substitution of zero for $\nabla^2 \phi_{i,j}$ and $\nabla^4 \phi_{i,j}$, and to Poisson's equation by substitution of $f(x_i, y_j)$ for $\nabla^2 \phi_{i,j}$ and $\nabla^2 f(x, y) \Big|_{\substack{x=x_i \\ y=y_i}}$ for $\nabla^4 \phi_{i,j}$. The truncation errors resulting from these substitutions are $O(h^6)$ for Laplace's equation and $O(h^4)$ for Poisson's equation.

Greenspan [7] developed a nine-point approximation to Laplace's equation for unequal spacing, that is, where the constant grid size h_1 in the x-direction is not the same as the constant grid size h_2 in the y-direction. The formula is

$$\begin{aligned} -20 \phi_{i,j} + 2 \left(\frac{S - r^2}{1 + r^2} \right) (\phi_{i+1,j} + \phi_{i-1,j}) + 2 \left(\frac{Sr^2 - 1}{1 + r^2} \right) (\phi_{i,j+1} + \phi_{i,j-1}) \\ + S_2 + O(h^6) \end{aligned} \quad (1.6)$$

One may note that for $r = 1$, i.e. $h_1 = h_2$, Eq. 1.6 reduces to Eq. 1.5 when applied to Laplace's equation.

The present work is a result of a computational study which was made on a nine-point approximation to the two-dimensional Poisson equation. This nine-point approximation, and the five-point approximation developed in Appendix A, were applied to several sample problems using the successive over-relaxation (SOR) iterative technique [5, 8, 9]. The error and speed of convergence of the approximations were then compared.

The nine-point approximation used is an adaptation of a general nine-point formula for the Laplacian operator developed by Rohach [10]. The approximation was given for unequal spacing. A parameter was defined which can be varied for reduced truncation error.

A similar computational study has been done by Holmes and Ettles [11] for the Reynolds' equation. The Reynolds' equation is a less commonly known elliptic partial differential equation which has applications for incompressible fluid flow, especially in the study of lubrication.

CHAPTER 2. THEORETICAL DEVELOPMENTS

A general nine-point relation for unequal spacing in two directions is given by Rohach [10]. In this work the relation will be expanded to a nine-point numerical approximation of the two-dimensional Poisson equation. Consider the relation (Fig. 2)

$$\left(\frac{1}{r} - p\right)\phi_{13} + (r - p)\phi_{24} + \frac{p}{2}\phi^{ii} - 2\left(\frac{1}{r} + r - p\right)\phi_0 \quad (2.1)$$

where

$$r = \frac{h_1}{h_2}$$

p = a parameter

$$\phi_{13} = \phi_1 + \phi_3$$

$$\phi_{24} = \phi_2 + \phi_4$$

$$\phi^{ii} = \phi^1 + \phi^2 + \phi^3 + \phi^4$$

To relate the derivatives to the respective finite differences, use the Taylor series expansion

$$\phi(x \pm h) = \phi(x) \pm h\phi'(x) + \frac{h^2}{2!}\phi''(x) \pm \frac{h^3}{3!}\phi'''(x) + \dots \quad (2.2)$$

Expanding each of the four axial points about the center point results in

$$\phi_1 = \phi_0 + h_1 \frac{\partial\phi_0}{\partial x} + \frac{h_1^2}{2!} \frac{\partial^2\phi_0}{\partial x^2} + \frac{h_1^3}{3!} \frac{\partial^3\phi_0}{\partial x^3} + \dots$$

$$\phi_3 = \phi_0 - h_1 \frac{\partial\phi_0}{\partial x} + \frac{h_1^2}{2!} \frac{\partial^2\phi_0}{\partial x^2} - \frac{h_1^3}{3!} \frac{\partial^3\phi_0}{\partial x^3} + \dots$$

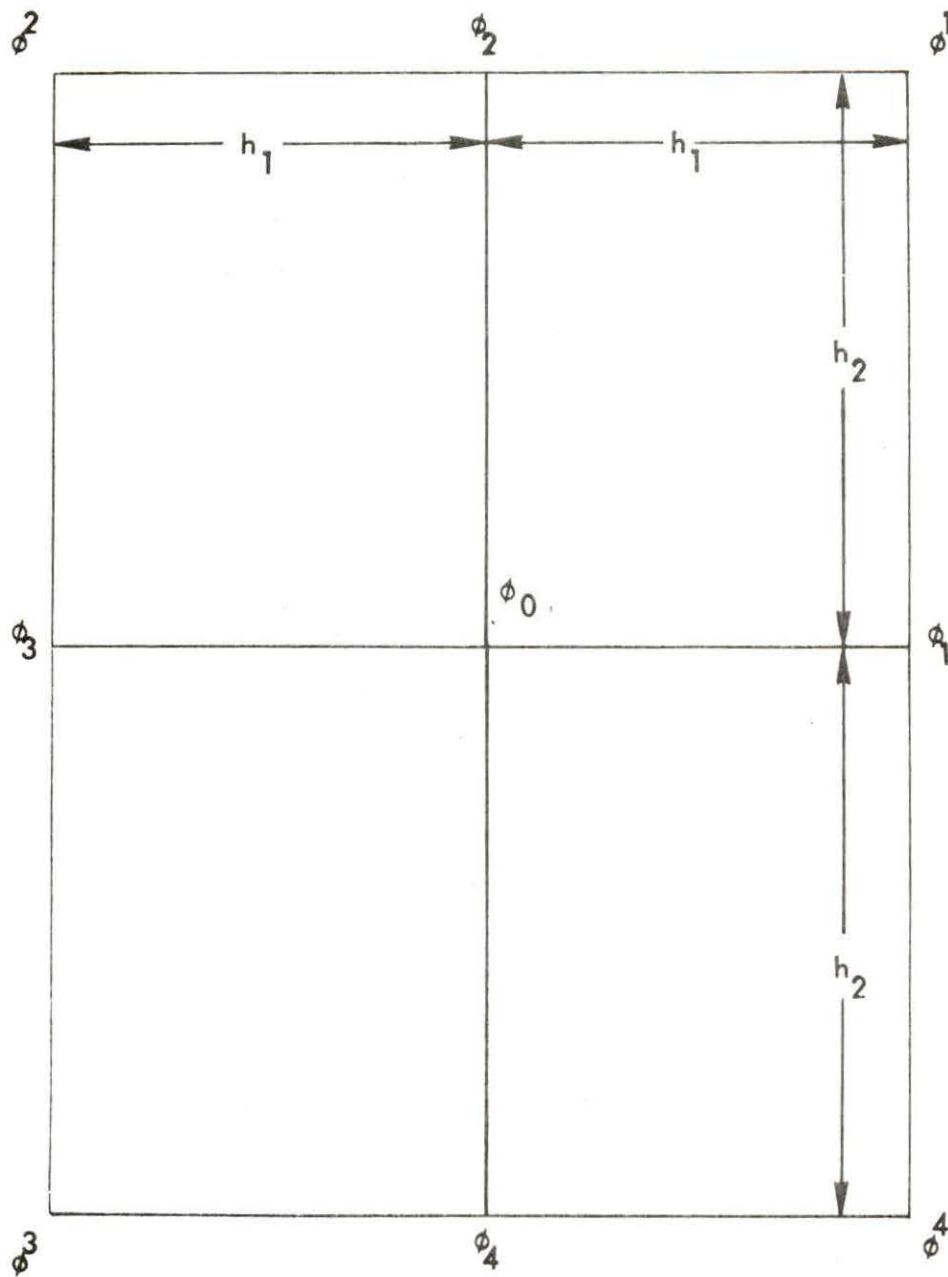


Fig. 2. Grid used for finite difference equation development.

$$\phi_2 = \phi_0 + h_2 \frac{\partial \phi_0}{\partial y} + \frac{h_2^2}{2!} \frac{\partial^2 \phi_0}{\partial y^2} + \frac{h_2^3}{3!} \frac{\partial^3 \phi_0}{\partial y^3} + \dots$$

$$\phi_4 = \phi_0 - h_2 \frac{\partial \phi_0}{\partial y} + \frac{h_2^2}{2!} \frac{\partial^2 \phi_0}{\partial y^2} - \frac{h_2^3}{3!} \frac{\partial^3 \phi_0}{\partial y^3} + \dots$$

By addition ϕ_{13} and ϕ_{24} become

$$\phi_{13} = \phi_1 + \phi_3 = 2(1 + \frac{\delta^2}{2!} + \frac{\delta^4}{4!} + \frac{\delta^6}{6!} + \dots)\phi_0 \quad (2.3)$$

$$\phi_{24} = \phi_2 + \phi_4 = 2(1 + \frac{\eta^2}{2!} + \frac{\eta^4}{4!} + \frac{\eta^6}{6!} + \dots)\phi_0 \quad (2.4)$$

where

$$\delta = h_1 \frac{\partial}{\partial x}, \quad \eta = h_2 \frac{\partial}{\partial y}$$

Expanding ϕ^1 about the center point results in

$$\begin{aligned} \phi^1 &= \phi_0 + (h_1 \frac{\partial \phi_0}{\partial x} + h_2 \frac{\partial \phi_0}{\partial y}) + \frac{1}{2!} (h_1 \frac{\partial \phi_0}{\partial x} + h_2 \frac{\partial \phi_0}{\partial y})^2 \\ &\quad + \frac{1}{3!} (h_1 \frac{\partial \phi_0}{\partial x} + h_2 \frac{\partial \phi_0}{\partial y})^3 + \dots \\ &= [1 + (\delta + \eta) + \frac{1}{2!} (\delta + \eta)^2 + \frac{1}{3!} (\delta + \eta)^3 + \dots]\phi_0 \end{aligned}$$

Similarly an expansion of the other corner points results in

$$\phi^2 = [1 + (\eta - \delta) + \frac{1}{2!} (\eta - \delta)^2 + \frac{1}{3!} (\eta - \delta)^3 + \dots]\phi_0$$

$$\phi^3 = [1 - (\delta + \eta) + \frac{1}{2!} (\delta + \eta)^2 - \frac{1}{3!} (\delta + \eta)^3 + \dots]\phi_0$$

$$\phi^4 = [1 + (\delta - \eta) + \frac{1}{2!} (\delta - \eta)^2 + \frac{1}{3!} (\delta - \eta)^3 + \dots]\phi_0$$

By addition ϕ^{ii} becomes

$$\begin{aligned}\phi^{ii} &= \phi^1 + \phi^2 + \phi^3 + \phi^4 = 4[1 + \frac{1}{2!} (\delta^2 + \eta^2) + \frac{1}{4!} (\eta^4 + 6\eta^2\delta^2 + \delta^4) \\ &+ \frac{1}{6!} (\eta^6 + 15\eta^4\delta^2 + 15\eta^2\delta^4 + \delta^6) + \dots]\phi_0\end{aligned}\quad (2.5)$$

Substitution of Eqs. 2.3, 2.4 and 2.5 into Eq. 2.1 results in

$$\begin{aligned}&(\frac{1}{r} - p)\phi_{13} + (r - p)\phi_{24} + \frac{p}{2} \phi^{ii} - 2(\frac{1}{r} + r - p)\phi_0 \\ &= [\frac{1}{r} (\delta^2 + r^2\eta^2) + \frac{1}{12r} (\delta^4 + 6rp\eta^2\delta^2 + r^2\eta^4) \\ &+ \frac{1}{360r} (\delta^6 + 15rp\eta^4\delta^2 + 15rp\eta^2\delta^4 + r^2\eta^6) + \dots]\phi_0 \\ &= h_1 h_2 [\nabla^2 + \frac{h_2^2}{12} (r^2 D_x^4 + 6rp D_{xy}^2 + D_y^4) \\ &+ \frac{h_2^4}{360} (r^4 D_x^6 + 15p(r D_{xyy}^2 + r^3 D_{xxy}^2) + D_y^6) + \dots]\phi_0\end{aligned}\quad (2.6)$$

where

$$D_x = \frac{\partial}{\partial x}, \quad D_y = \frac{\partial}{\partial y}, \quad D_{xy} = \frac{\partial^2}{\partial x \partial y}, \text{ etc.}$$

Solving Eq. 2.6 for $\nabla^2 \phi_0$, one has a general nine-point approximation to the Laplacian operator

$$\begin{aligned}\nabla^2 \phi_0 &= \frac{1}{h_1 h_2} [(\frac{1}{r} - p)\phi_{13} + (r - p)\phi_{24} + \frac{p}{2} \phi^{ii} - 2(\frac{1}{r} + r - p)\phi_0] \\ &- \frac{h_2^2}{12} (r^2 D_x^4 + 6rp D_{xy}^2 + D_y^4) + O(h^4)\end{aligned}\quad (2.7)$$

The truncation error for this relation is determined by the proper choice of p . It can be seen that the normal five-point relation (Eq. 1.4) occurs for $p = 0$. In order to get a truncation error of $O(h^4)$ it is necessary for

$$(r^2 D_x^4 + D_y^4 + 6rp Dxy^2)\phi_0 = 0 \quad (2.8)$$

Rearranging Eq. 2.8 into

$$\begin{aligned} (r^2 D_x^4 + D_y^4 + 6rp Dxy^2)\phi_0 &= (6rp - r^2 - 1) Dxy^2 \phi_0 \\ &+ (r^2 D_x^2 + D_y^2) \nabla^2 \phi_0 = 0 \end{aligned}$$

and solving for p results in

$$p = \frac{r + \frac{1}{r}}{6} - \frac{(r^2 D_x^2 + D_y^2) \nabla^2 \phi_0}{6r Dxy^2 \phi_0} \quad (2.9)$$

For Laplace's equation $\nabla^2 \phi_0 = 0$, resulting in

$$p = \frac{r + \frac{1}{r}}{6} \quad (2.10)$$

Substitution of Eq. 2.10 into Eq. 2.7 results in

$$(5 - r^2)\phi_{13} + (5r^2 - 1)\phi_{24} + \frac{1}{2}(r^2 + 1)\phi^{ii} - 10(1 + r^2)\phi_0 = 0 \quad (2.11)$$

Multiplication of Eq. 2.11 by $\frac{2}{r^2 + 1}$ gives Greenspan's relation [7],

Eq. 1.6. For the case of equal spacing ($r = 1$) Eq. 2.10 becomes

$$p = \frac{1}{3} \quad (2.12)$$

Substitution of Eq. 2.12 for p in Eq. 2.7 results in the nine-point relation developed by Bickley [1] and others [2, 3, 4, 5, 6].

However in equations where $\nabla^2 \phi_0$ does not vanish, $Dxy^2 \phi_0$ cannot be found explicitly. For these cases consider the numerical approximation

$$D_{xy}^2 \phi_0 = \left(\frac{1}{h_1 h_2}\right)^2 (\phi^{ii} - 2\phi_{ii} + 4\phi_0) + O(h^2) \quad (2.12)$$

where

$$\phi_{ii} = \phi_{13} + \phi_{24}$$

$$\phi^{ii} = \phi^1 + \phi^2 + \phi^3 + \phi^4 \quad \text{corners}$$

The resulting truncation error goes into the next error term in Eq. 2.7.

With the use of this approximation Eq. 2.9 becomes

$$p = \frac{r + \frac{1}{r}}{6} - \frac{(h_1 h_2)^2 (r^2 D_x^2 + D_y^2) \nabla^2 \phi_0}{6r(\phi^{ii} - 2\phi_{ii} + 4\phi_0)} \quad (2.13)$$

Now p can be readily evaluated for Poisson's equation by the substitution of the known function $f(x, y)_0$ for $\nabla^2 \phi_0$. The resulting relation, which was used for this study, is

$$f(x, y)_0 = \frac{1}{h_1 h_2} \left[\left(\frac{1}{r} - p\right) \phi_{13} + (r - p) \phi_{24} + \frac{p}{2} \phi^{ii} - 2\left(\frac{1}{r} + r - p\right) \phi_0 \right] + O(h^4) \quad (2.14)$$

where

$$p = \frac{r + \frac{1}{r}}{6} - \frac{(h_1 h_2)^2 (r^2 D_x^2 + D_y^2) f(x, y)_0}{6r(\phi^{ii} - 2\phi_{ii} + 4\phi_0)} \quad (2.15)$$

For problems where the derivatives in the numerator of Eq. 2.15 are difficult to evaluate a further numerical approximation can be used. The derivatives can be approximated as :

$$(r^2 D_x^2 + D_y^2) f_0 = \frac{r^2}{h_1^2} (f_{i+1,j} - 2f_{i,j} + f_{i-1,j}) + \frac{1}{h_2^2} (f_{i,j+1} - 2f_{i,j} + f_{i,j-1}) + O(h^2) \quad (2.16)$$

central difference
of f

This
approximation
should
be smooth

where

$$f_0 = f(x, y) \Big|_{\substack{x=x_0 \\ y=y_0}}$$

Again the truncation error goes into the next error term. In this study p was calculated using Eq. 2.15 with either exact or numerical values for $(r^2 D_x^2 + D_y^2)f_0$, giving results which will be discussed later.

CHAPTER 3. COMPUTATIONAL PROCEDURES

3.1 Analytical Solutions

To compare the accuracy of the nine-point relation developed in Chapter 3 with the five-point relation from Appendix A it is necessary to use a configuration of Poisson's equation with an exact analytical solution. However there are very few configurations of Poisson's equation with solutions that could be easily applied to this study. For this reason simple analytical solutions $\phi(x, y)$ were assumed initially. The configurations of Poisson's equation for those solutions were then found by substitution of $\phi(x, y)$ into the general form of Poisson's equation followed by differentiation for the function $f(x, y)$.

There were many possible solutions which could have been initially assumed. However in this study attempts were made to handle at least one of each of the three ³ general forms that a solution to a differential equation can take, that is, trigonometric, exponential ² or hyperbolic, and ³ polynomial. The solutions were applied to, and approximated over simple two dimensional rectangular regions. The regions had constant grid spacing, although not always equal spacing in each direction.

The function $\phi(x, y) = \sin(xy)$ was chosen to represent the trigonometric functions. The values of x and y ranged from 0.5 to 1.5 for most cases and from 0.1 to 1.1 for others. These values of x and y for the rectangular region gave a function which gradually increased from the lower left corner to a maximum near the upper right corner, as can be seen in Fig. 3. Poisson's equation for this assumed solution is

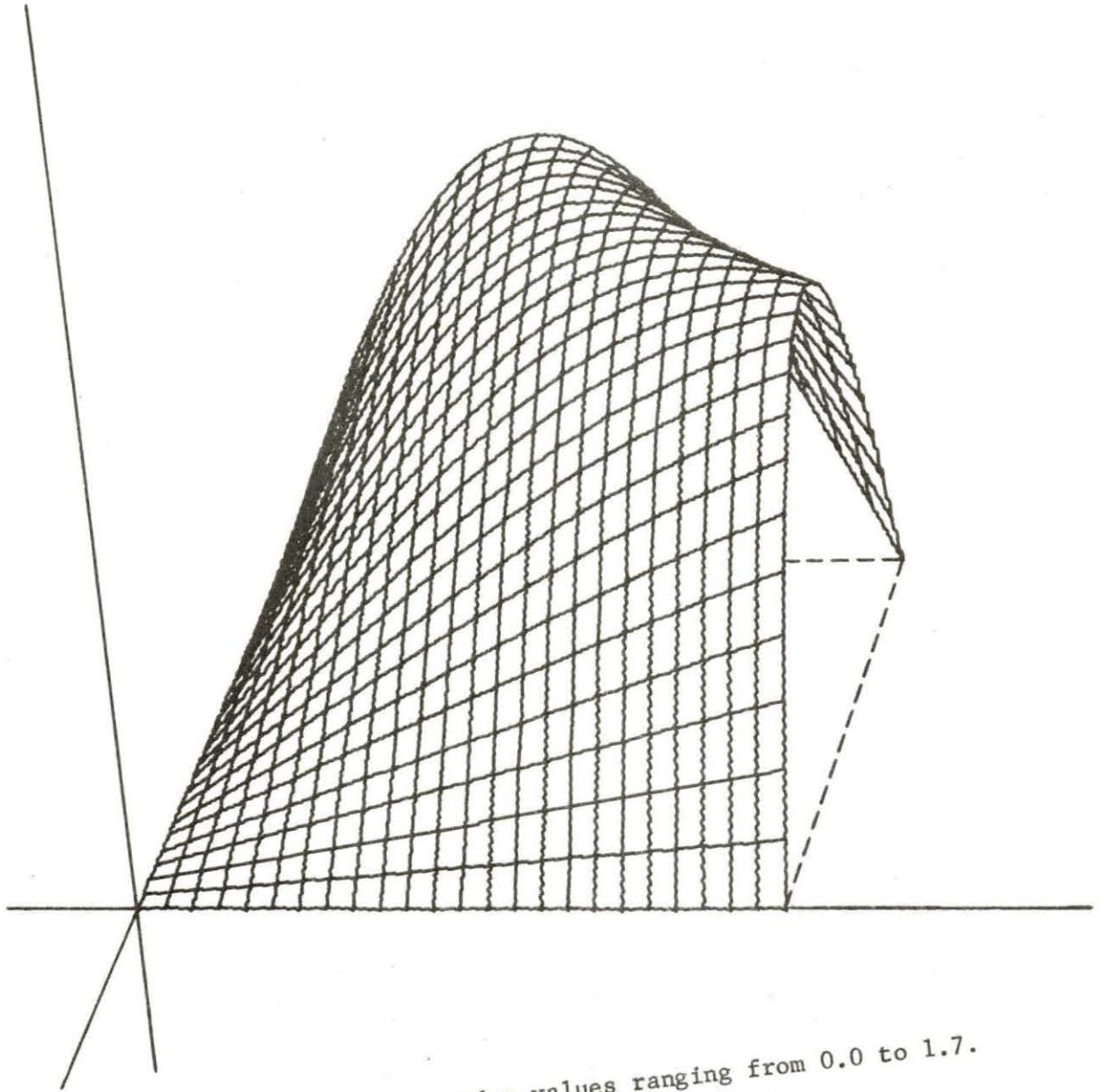


Fig. 3. Plot of $\sin(xy)$ for x and y values ranging from 0.0 to 1.7.

$$\nabla^2 \phi(x, y) = (x^2 + y^2) \sin(xy) \quad (3.1)$$

To represent exponential solutions a hyperbolic function was chosen, $\phi(x, y) = 1 + \sinh(xy)$. For this function two ranges of x and y values were again used, one from -0.25 to 0.75 and the other from 0.0 to 1.0. Unity was added to $\sinh(xy)$ to avoid zero values for $\phi(x, y)$, which would have led to division by zero in the relative error calculations. These will be discussed in the next section. The three dimensional view of this function over the rectangular region used can be seen in Fig. 4. Poisson's equation for this assumed hyperbolic solution is

$$\nabla^2 \phi(x, y) = (x^2 + y^2) \sinh(xy) \quad (3.2)$$

Several polynomial solutions were considered, the three actually used in the study were $\phi(x, y) = x^4 + y^3$, $\phi(x, y) = x^2 + y^2 - 2x^2y^2$ and $\phi(x, y) = x^4 + y^2 - 2x^3y^2$. They were applied using values of x and y ranging from 0.0 to 1.0 over the region. The majority of work was done with the third function $x^4 + y^2 - 2x^3y^2$. It is shown in Fig. 5 for the x and y values used. Poisson's equation for this same equation is

$$\nabla^2 \phi(x, y) = 12x^2 - 2xy^2 - 4x^3 + 2 \quad (3.3)$$

The function $x^4 + y^3$ was the first polynomial applied. It illustrated a limitation of the nine-point technique used. A function that is to be approximated must be of a form such that the cross derivative in the denominator of Eq. 2.9 is not zero. If this

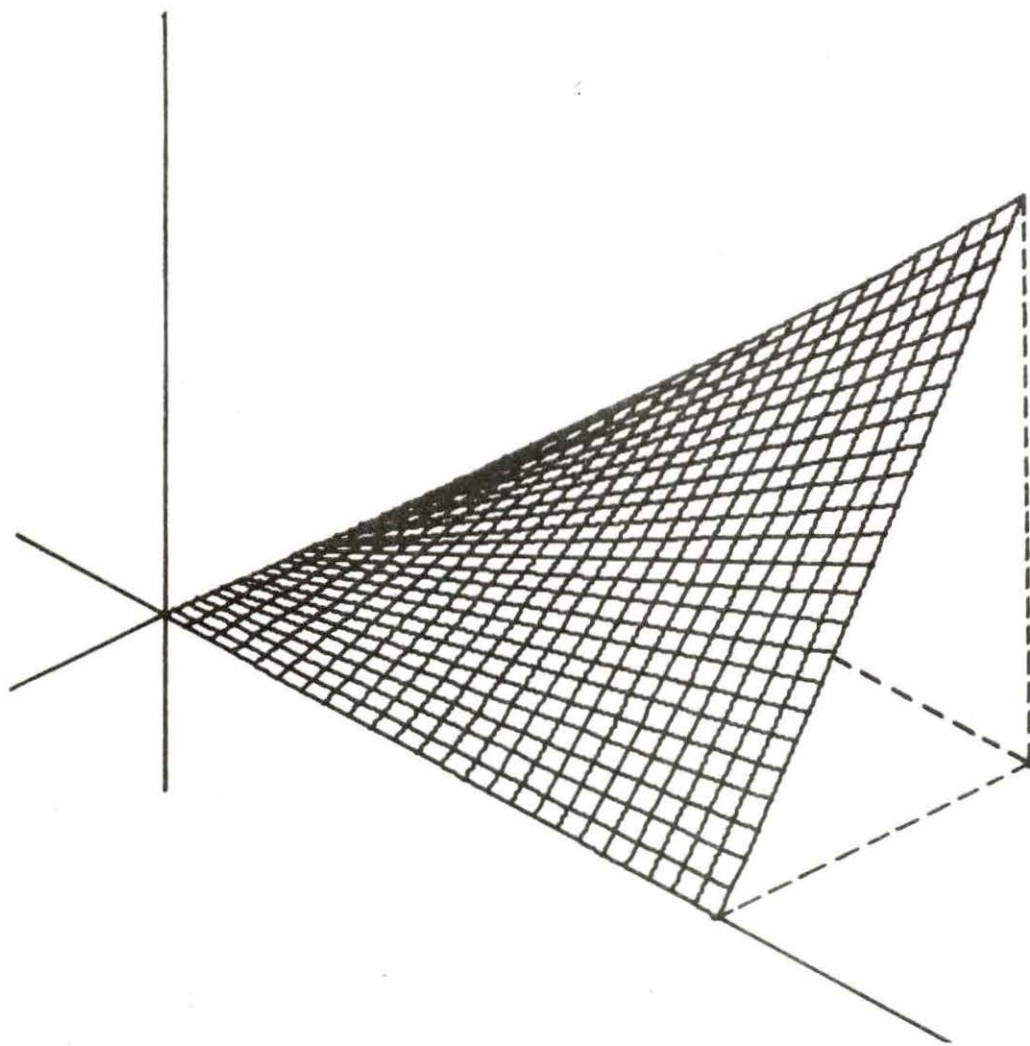


Fig. 4. Plot of $1 + \sinh(xy)$ for x and y values ranging from -0.25 to 0.75.

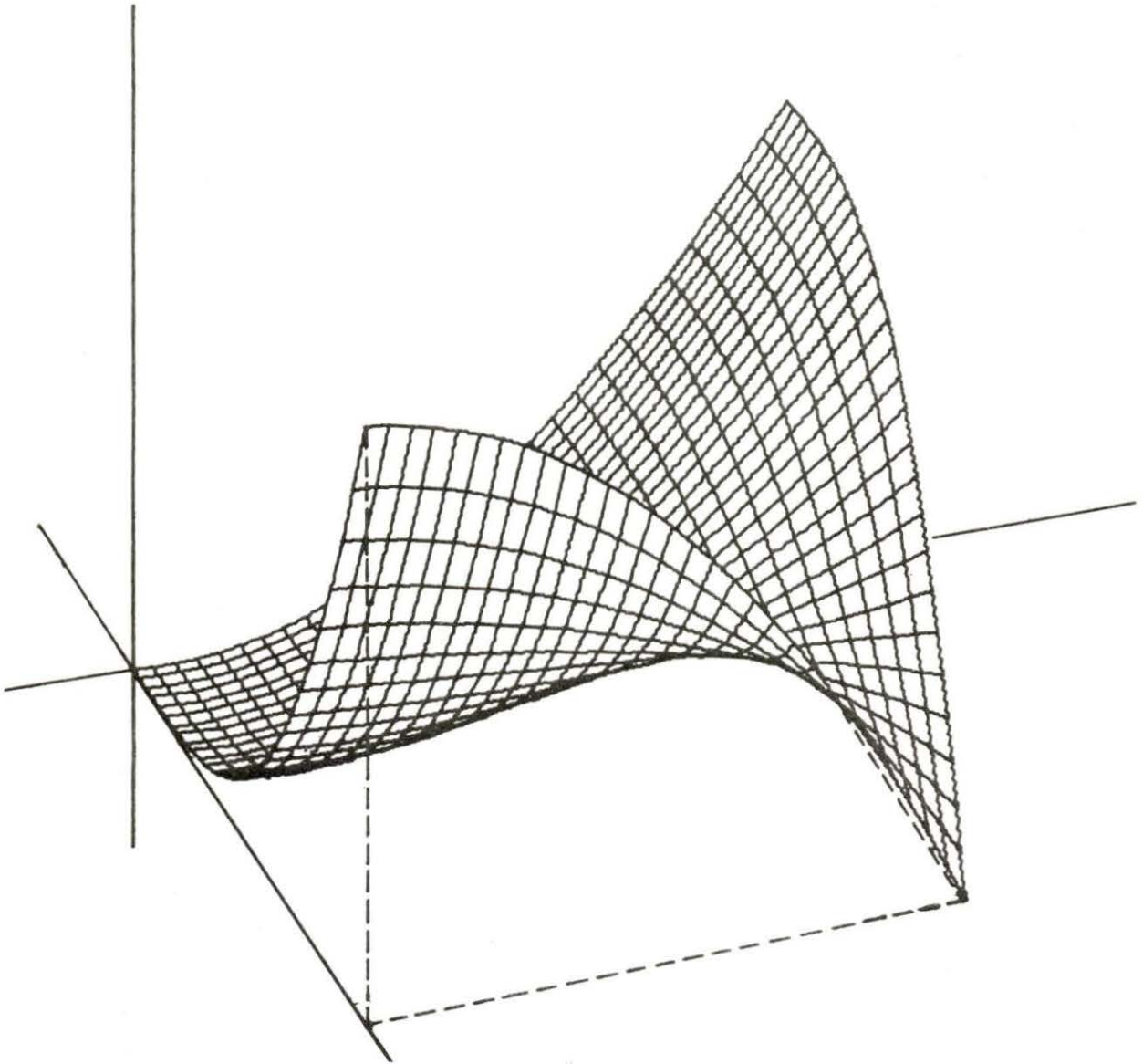


Fig. 5. Plot of $x^4 + y^2 - 2x^3y^2$ for x and y values ranging from 0.0 to 1.0.

derivative is zero the finite difference relation approximating the derivative approaches zero, causing the second term of Eq. 2.9 to approach infinity, which in turn leads to nonconvergence of the solution. However the importance of this limitation is questionable, very few solutions to Poisson's equation take the form of simple polynomials. Most polynomial solutions are infinite series, for which the derivative in question would not be zero.

What is order of Truncation error?

3.2 Definitions of Error

The assumed analytical solutions to Poisson's equation just discussed can be used to evaluate the absolute and relative error in numerical solutions to the same Poisson's equation. If $\phi_{i,j}$ is the value of the analytical solution at a point (i, j) , and $\phi_{i,j}^*$ is the value of the numerical solution at the same point, then the absolute error at point (i, j) is defined as

$$e_{a_{i,j}} = |\phi_{i,j} - \phi_{i,j}^*| \quad (3.4)$$

and the relative error at point (i, j) is defined as

$$e_{r_{i,j}} = \frac{|\phi_{i,j} - \phi_{i,j}^*|}{\phi_{i,j}} \quad (3.5)$$

To arrive at a single overall error value for the numerical solution the l_2 or Euclidean norms [12] for the absolute and relative error matrices can be calculated. The Euclidean error norm used in this study is defined as

$$E_{l_2} = [\sum_i \sum_j |e_{i,j}|^2]^{1/2} \quad (3.6)$$

In this study the analytical solution was calculated at each of the grid points using the assumed solutions. Because all calculations in the study were made using Fortran double precision variables the analytical solution was accurate to approximately sixteen places. Thus for all practical purposes the analytical solution calculated by the computer could be taken as exact. This exact solution was used to evaluate the l_2 error norms, both absolute and relative for the nine- and five-point numerical solutions.

3.3. Speed of Convergence and SOR Optimization

When solving finite difference equations with an iterative technique, the principal interest is that the iterated function converges to the solution as fast as possible. Therefore in a comparison of two different finite difference techniques one must have an accurate method for determining the speed of convergence of the techniques. The first inclination would be to use the number of iterations to convergence as a measure of speed of convergence. However this does not always give accurate results.

A more accurate method involves the calculation of the convergence rate defined as [9]

$$\nu = -\ln \lambda_1 \quad (3.7)$$

where

ν = the convergence rate

λ_1 = the largest eigenvalue of the iteration matrix.

The eigenvalue λ_1 can be calculated using the ratio of two successive l_2 residual norms, that is

$$\lambda_1 = \frac{\|r^p\|}{\|r^{p+1}\|} \quad (3.8)$$

The l_2 residual norms are defined as

$$\|r\| = [\sum_i \sum_j (r_{i,j})^2]^{1/2} \quad (3.9)$$

Where the residual $r_{i,j}$ is defined as

$$r_{i,j}^{(p)} = \phi_{i,j}^{(p+1)} - \phi_{i,j}^{(p)} \quad (3.10)$$

where

$\phi_{i,j}$ = numerical solution at point (i, j)

p = iterate number, ($p = 0, 1, 2, 3, \dots$)

However, the application of Eq. 3.8 to iterative schemes solved using the successive over-relaxation technique may lead to some difficulty in calculations of λ_1 using Eq. 3.7. As α , the over-relaxation parameter for the SOR technique, approaches its optimum value the successive values of λ_1 , calculated using Eq. 3.8, behave erratically. This makes it difficult to find a constant value of λ_1 for use in Eq. 3.7.

The erratic behavior of λ_1 can be solved by using a graphical method for calculating the convergence rate. For this graphical method the successive $\log l_2$ residual norms are plotted versus the number of the respective iterate. This results in a straight or nearly straight line with a negative slope (Fig. 6). Each value of α

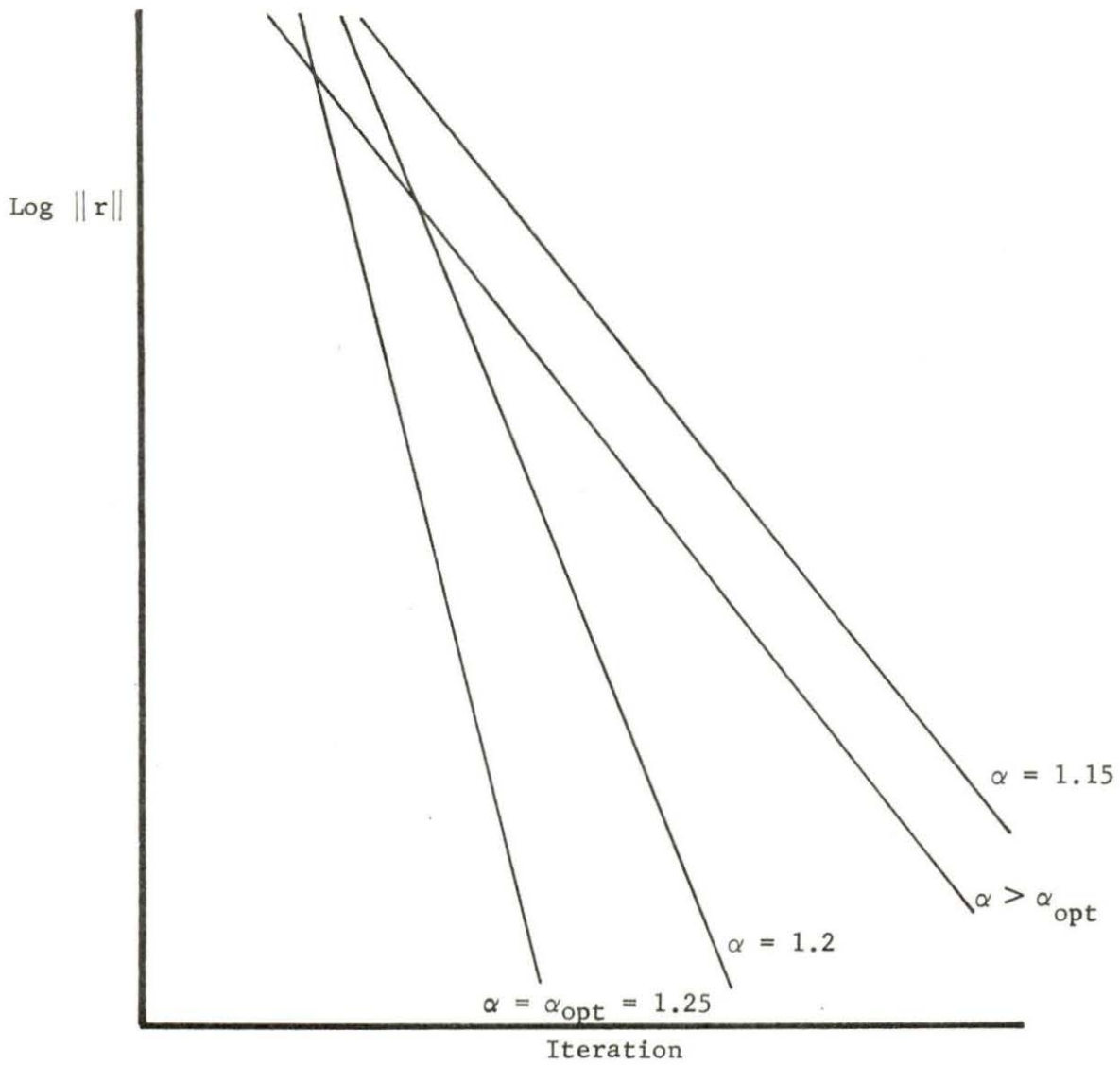


Fig. 6. Plot of $\log l_2$ residual norm vs iteration for several α values.

produces its own individual curve, and as α approaches its optimum value the lines become successively steeper, up to $\alpha > \alpha_{\text{opt}}$ where the trend reverses (Fig. 6).

It can be shown that the absolute value of the slope of one of these lines is the convergence rate of the solution for the α corresponding to that line. However this method while accurate can be quite tedious if applied to studies requiring optimization of α . In this study a least squares fit to the $\log \|r\|$ vs iteration curves was used. The convergence rate could then be directly calculated from the slope of this fitted curve. How

The curve fitting was accomplished as the l_2 residual norms were calculated at the end of each iteration. Thus the slope of the fitted curve and therefore the convergence rate for that value of α could be calculated directly by the same program that solved the difference equations. Because trial and error is the only method available for optimization of α the direct calculation of the convergence rate made the optimization process much simpler.

Another aid to the time consuming optimization process was the use of a plot of λ_1 vs α . An example of such a plot is shown in Fig. 7. It can be seen in this plot that up to α_{opt} λ_1 decreases as α increases, and beyond α_{opt} λ_1 increases rapidly with α . Because such plots make the general trend of λ_1 with α more easily seen better choices of α can be made during the trial and error search for α_{opt} , thus reducing the number of calculations required.

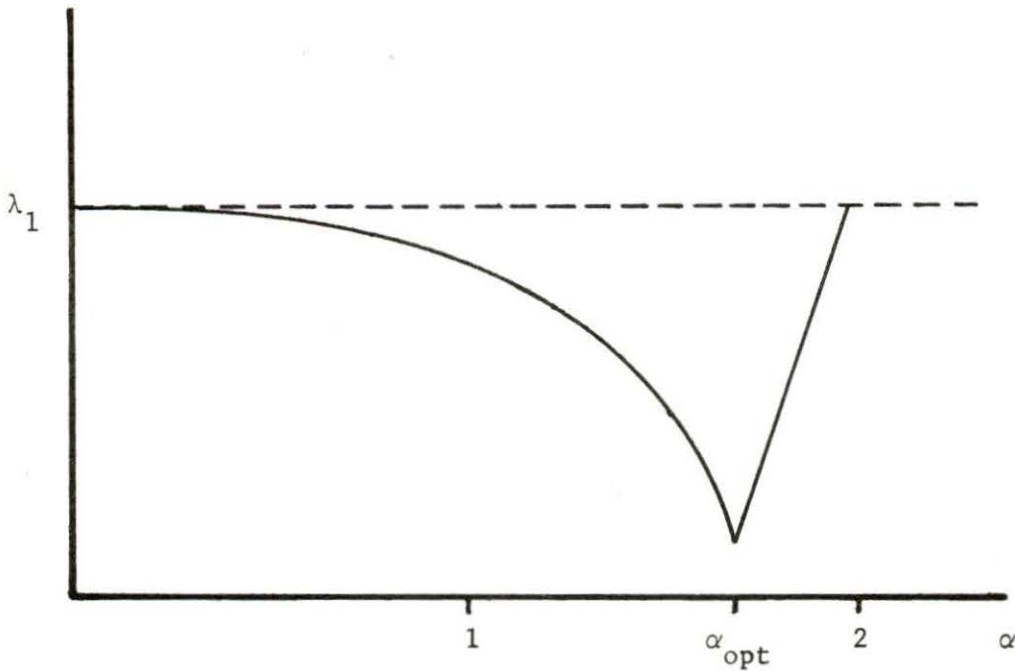


Fig. 7. Plot of λ_1 vs the over-relaxation parameter.

3.4 Description of Boundary Conditions

As discussed in Chapter 1 the boundary conditions for an elliptic partial differential equation are made up of either the function ϕ , its normal derivative, or a linear combination of both. Because the analytical solution $\phi(x, y)$ was assumed initially, any of these boundary conditions could have been used for this study. However since $\phi(x, y)$ was already being calculated for the error evaluation it seemed easiest to just use the function $\phi(x, y)$ for the boundary conditions.

The conditions were set up by first calculating the analytical solution $\phi(x, y)$ for the entire region being used. Then all the mesh points of the region were set equal to zero except for the boundary points, which were left equal to the appropriate values of $\phi(x, y)$.

Thus the initial conditions for the problems solved in this study were boundary points equal to $\phi(x, y)$ and all interior points equal to zero.

3.5 Description of Computer Program Used for Study

The computer program used was specifically designed and written for the purposes of this study. The program was used for comparison of the error and speed of convergence of two finite difference techniques. It was written in Fortran IV language for a Watfiv compiler, and consisted of a main program along with several sub-routines. A short description will be given here along with a simplified flowchart in Appendix B.

The purpose of the main program is to act as a source deck for supplying information required in common by both finite difference calculations. The main program, through the use of input information, sets up and dimensions the region to be used for the calculations. It is designed to set up rectangular regions of either regular or irregular shape, an example of the later is shown in Fig. 8. The values of h_1 and h_2 , along with the x and y values for each grid point, are also calculated for the region.

These x and y values are then used to calculate the analytical solutions described in Sec. 3.1, the function $f(x, y)$ from Poisson's equation, and the numerator of Eq. 2.15. Finally the main program, through the use of a short subroutine, establishes the boundary conditions described in Sec. 3.4. These boundary conditions along with the

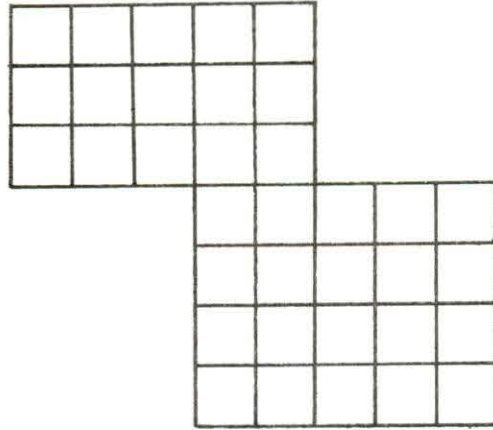


Fig. 8. Irregular rectangular region.

values for the analytical solution, $f(x, y)$ and the numerator of Eq. 2.15 are passed, using two dimensional arrays, to the subroutines containing the finite difference calculations.

Upon completion of all the necessary calculations, the main program calls the subroutine with the five-point calculation. This subroutine, with the boundary conditions passed to it from the main program, solves the system of five-point difference equations using the iterative SOR technique. As this solution proceeds the l_2 residual norms and values of λ_1 are calculated for each iteration. At an iteration designated by an input parameter the curve fit of λ_1 described in Sec. 3.3 begins. After the solution has converged¹ the value of the convergence rate ν is calculated from the curve fit data. The analytical solution calculated in the main program is then used to calculate the absolute and relative error in the approximate solution, as described in Sec. 3.2.

¹Convergence is measured by the difference between two successive l_2 residual norms. The solution is said to have converged when this difference is less than a predetermined value.

The subroutine containing the nine-point calculation is called by the main program after the five-point calculation is completed. The solution of the nine-point difference equations proceeds in essentially the same manner as that of the five-point equations. The error and convergence rate calculations are also handled in the same manner as the five-point values. The only real difference in the two subroutines is the additional calculation of the parameter p (Eq. 2.15) required for the nine-point relation. This calculation for p at each interior mesh point also requires the solution of a system of difference equations. This system like the nine- and five-point systems is solved using the iterative SOR technique. The nine-point subroutine is set up such that the value of p could be calculated for each iteration, or at regular intervals during the solution.

CHAPTER 4. RESULTS AND DISCUSSION

4.1 Introduction

As stated previously, the objective of this study was the comparison of two finite difference relations, the nine-point relation developed in Chapter 2 and the usual five-point relation. The comparison was made to show the higher accuracy of the nine-point relation and to determine which relation converged more rapidly. In addition, through the comparison of the error and speed of convergence, an attempt was made to show a computational advantage for the use of the nine-point relation.

In the study it was attempted to show that the accuracy of a five-point solution to a problem could be achieved using the nine-point relation with many fewer points. Further it was attempted to show that when applied in this manner, the nine-point relation would converge more rapidly than the five-point relation. Therefore the nine-point relation applied in this manner would give the advantages of needing less computer storage area and less computation time. Further these advantages would be gained while still providing the accuracy of a five-point solution which is more than adequate for most practical applications.

4.2 Error Analysis Results

In order to make the analysis just discussed, it was necessary to relate the accuracy of the numerical solution to the number of grid points used. This was done through the use of a logarithmic plot

of the l_2 error norm as a function of the grid spacing, which is directly related to the number of grid points. For regions with equal spacing the absolute error norms were plotted as a function of h , where $h = h_1 = h_2$. For regions with unequal spacing the absolute error norms were plotted as a function of R , where $R = \sqrt{h_1^2 + h_2^2}$ as suggested by Holmes and Ettles [11].

To generate the data necessary for such plots numerical solutions of a problem applied to several different regions were calculated. The regions were of constant shape and size, and had the same range of x and y values. They differed only in the number of grid points used for each calculation. Thus from these numerical solutions, specific error values could be calculated for each of a series of h or R values.

As discussed in Section 3.1, three assumed solutions were to be analyzed in this study. An attempt was made to apply the above analysis to all three types of functions. They were applied using square regions with sides of length unity to allow consistent and easy calculation of h from the number of grid points. The functions were applied using both equal and unequal spacing for the regions.

For reasons to be discussed later, the error analysis was completed only for the sine and hyperbolic functions. They were applied using two ranges of x and y values for each function, 0.1 to 1.1 and 0.5 to 1.5 for the sine function, and - 0.25 to 0.75 and 0.0 to 1.0 for the hyperbolic function. For the application of the functions to equally spaced regions, eight values of the absolute error norm were calculated, one for each of the grids ranging from 5 x 5 to 12 x 12. Six values were calculated for the unequally spaced regions, which had grids ranging

from 5×7 to 10×11 . To ensure that the residual error was negligible compared to the absolute error, the iterative procedure was continued until the l_2 residual norm had fallen to below 10^{-10} .

The problems evaluated in this study were chosen to avoid a large range of values of the function; most values of $\phi(x, y)$ ranged between 0 and 1 with a few ranging as high as 2. Because of the small ranges of values, it was felt that the increased weighting would not be large if the absolute error was used. Further it was found that the relative error did not vary significantly from the absolute error as can be seen in Fig. 9. This small difference in the actual values of absolute and relative error, together with the feeling that the uneven weighting would not be important, led to the use of the absolute error.

The majority of the error calculations were made without an attempt at optimization of the SOR over-relaxation parameter α . This was due to the length of time required for optimization, and because the error is not a function of α . Instead a constant value of $\alpha = 1.15$ was used for both the five- and nine-point calculations. For the convergence of the solution, some cases also required either under- or over-relaxation of the SOR calculation of Eq. 2.15. Optimization was attempted only for the sine function with x and y values of 0.5 to 1.5, the results of this optimization will be discussed in Section 4.4.

The logarithmic plots of absolute error vs h for the calculations made with various configurations of the sine and hyperbolic functions are shown in Figs. 10 through 16. In each of these figures are illustrated

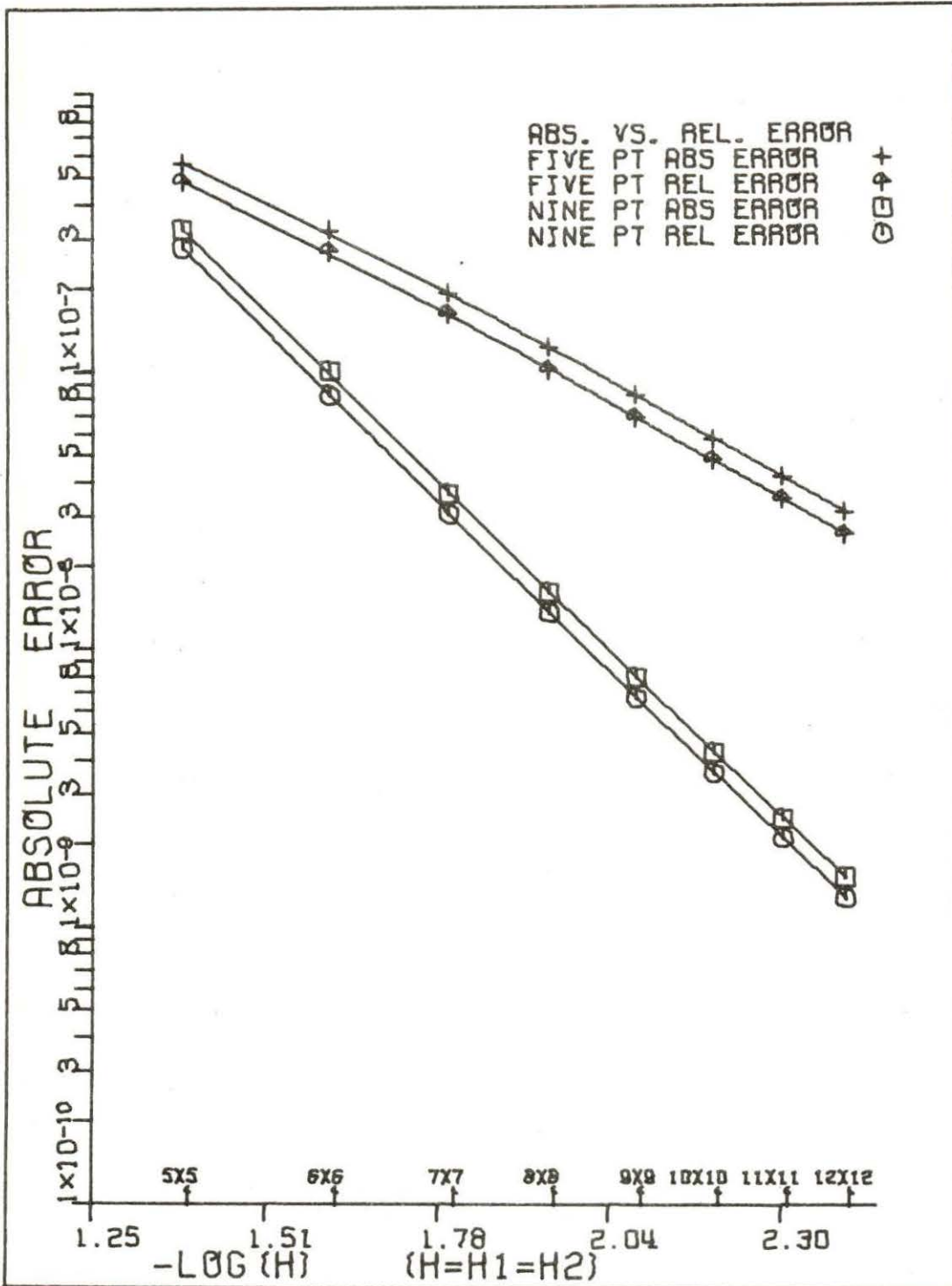


Fig. 9. Plot of absolute and relative error for a configuration using $\phi = 1 + \sinh(xy)$.

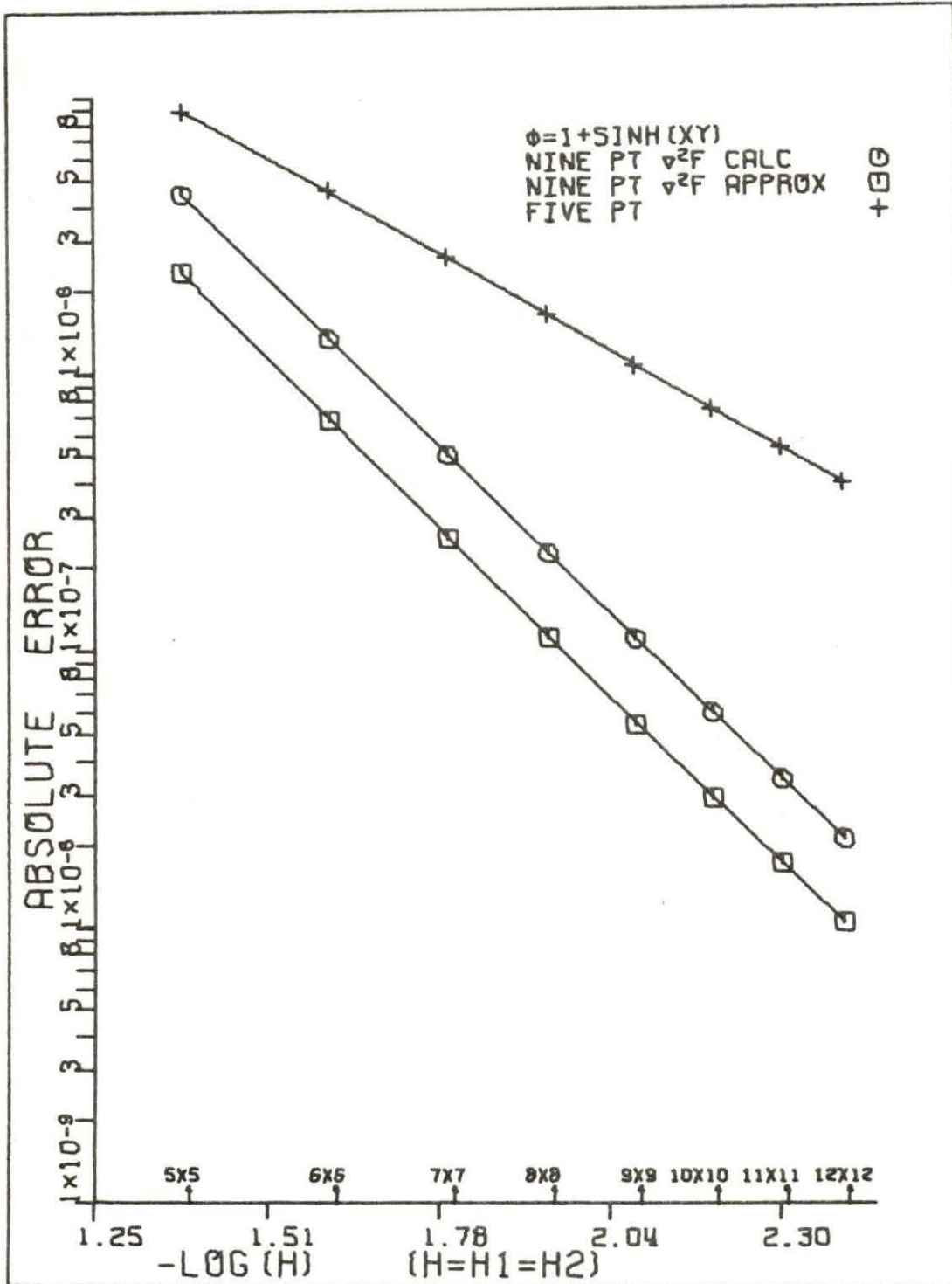


Fig. 10. Plot of absolute error as a function of grid spacing h , for $\phi = 1 + \sinh(xy)$ with x and y values ranging from 0.0 to 1.0.

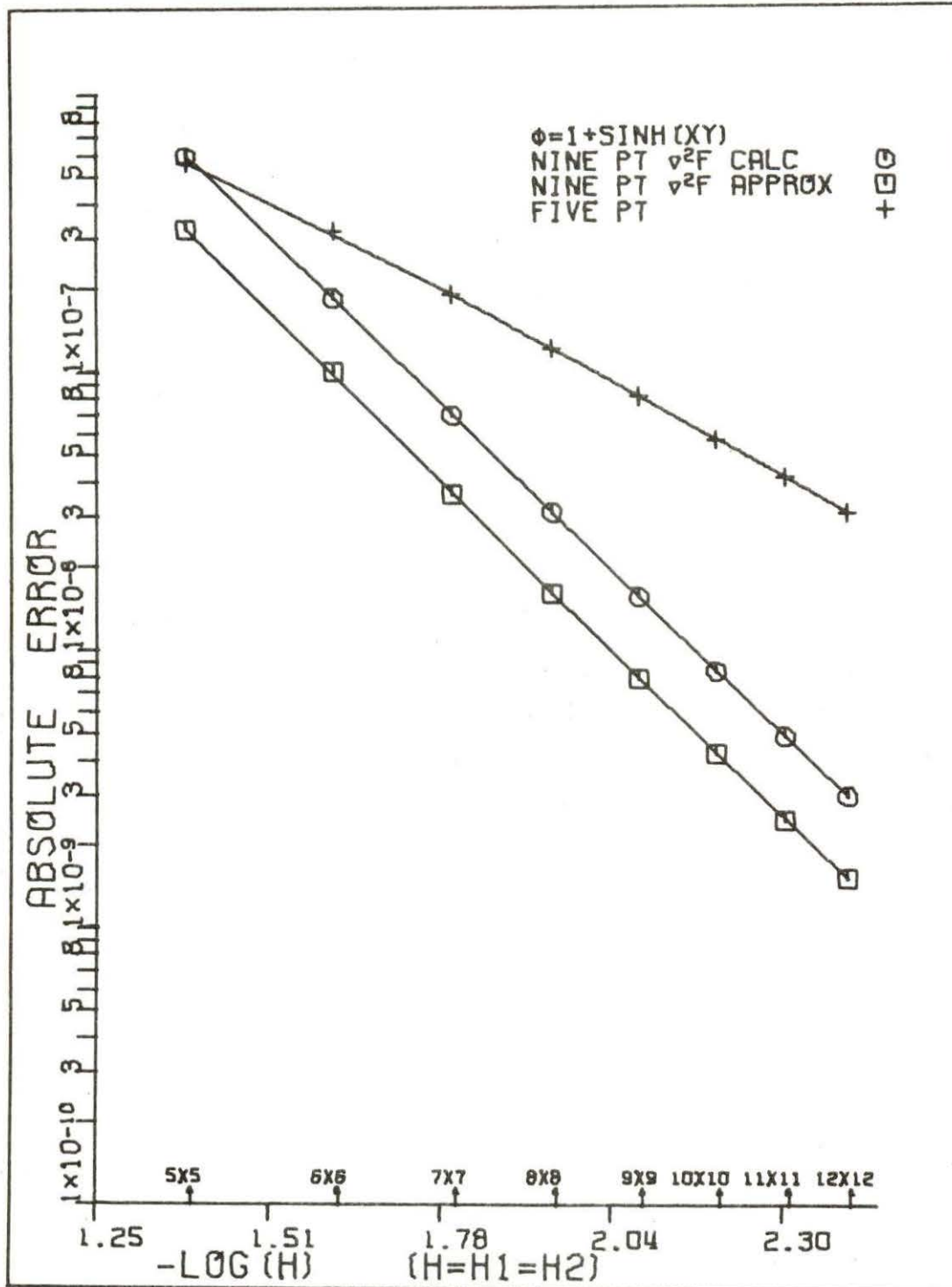


Fig. 11. Plot of absolute error as a function of grid spacing h , for $\phi = 1 + \sinh(xy)$ with x and y values ranging from -0.25 to 0.75 .

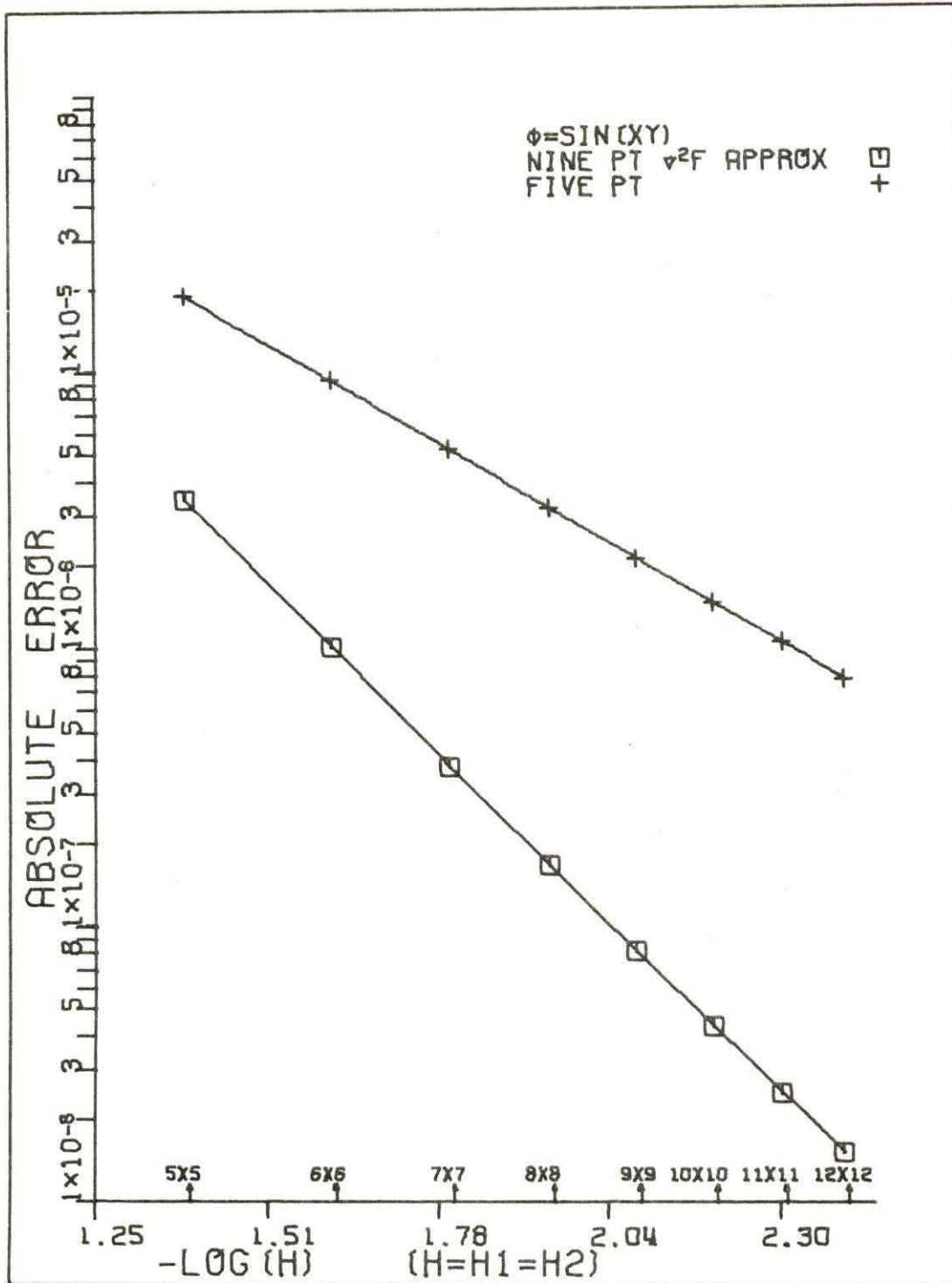


Fig. 12. Plot of absolute error as a function of grid spacing h , for $\phi = \sin(xy)$ with x and y values ranging from 0.1 to 1.1.

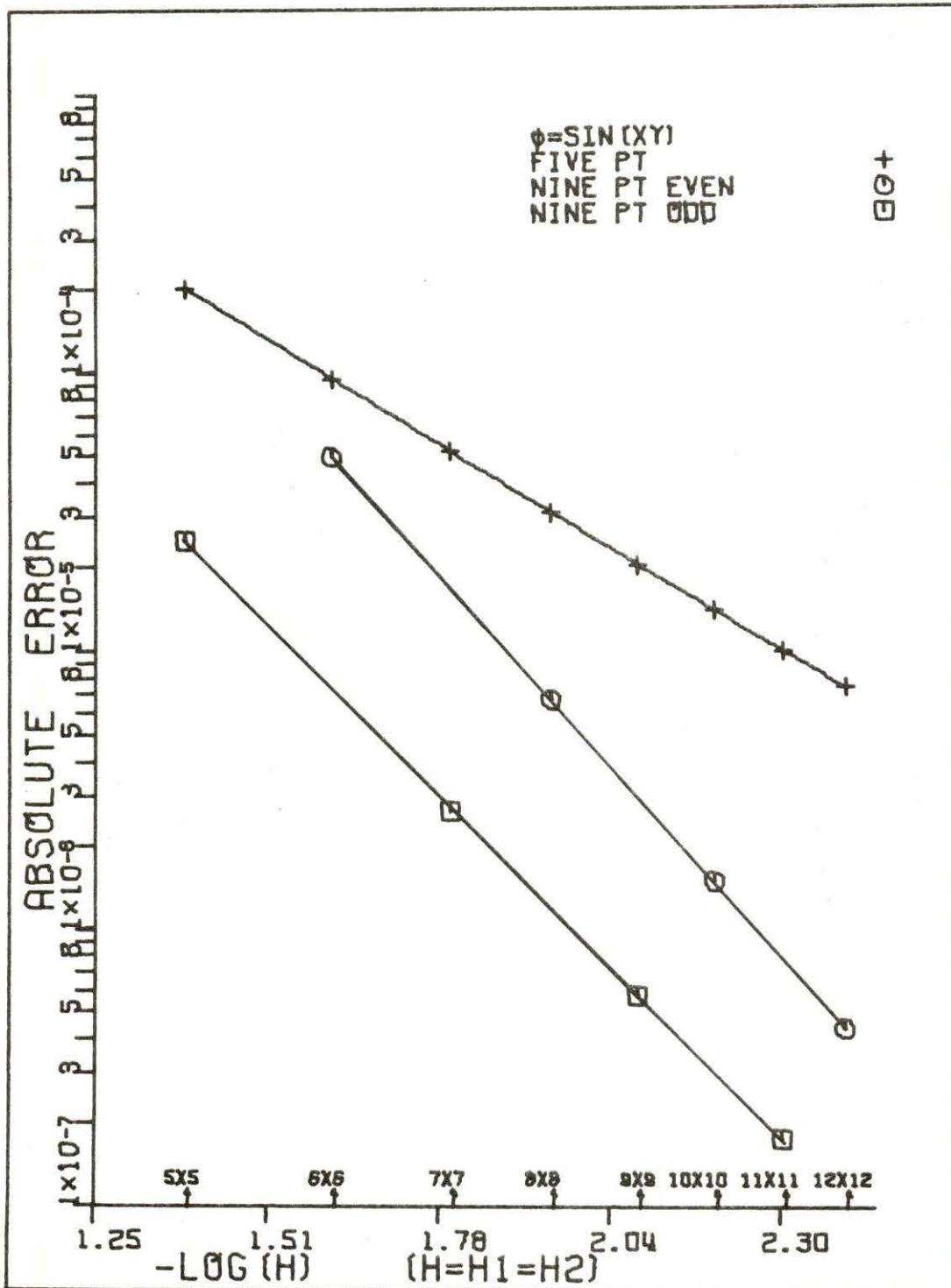


Fig. 13. Plot of absolute error as a function of grid spacing h , for $\phi = \sin(xy)$ with x and y values ranging from 0.5 to 1.5.

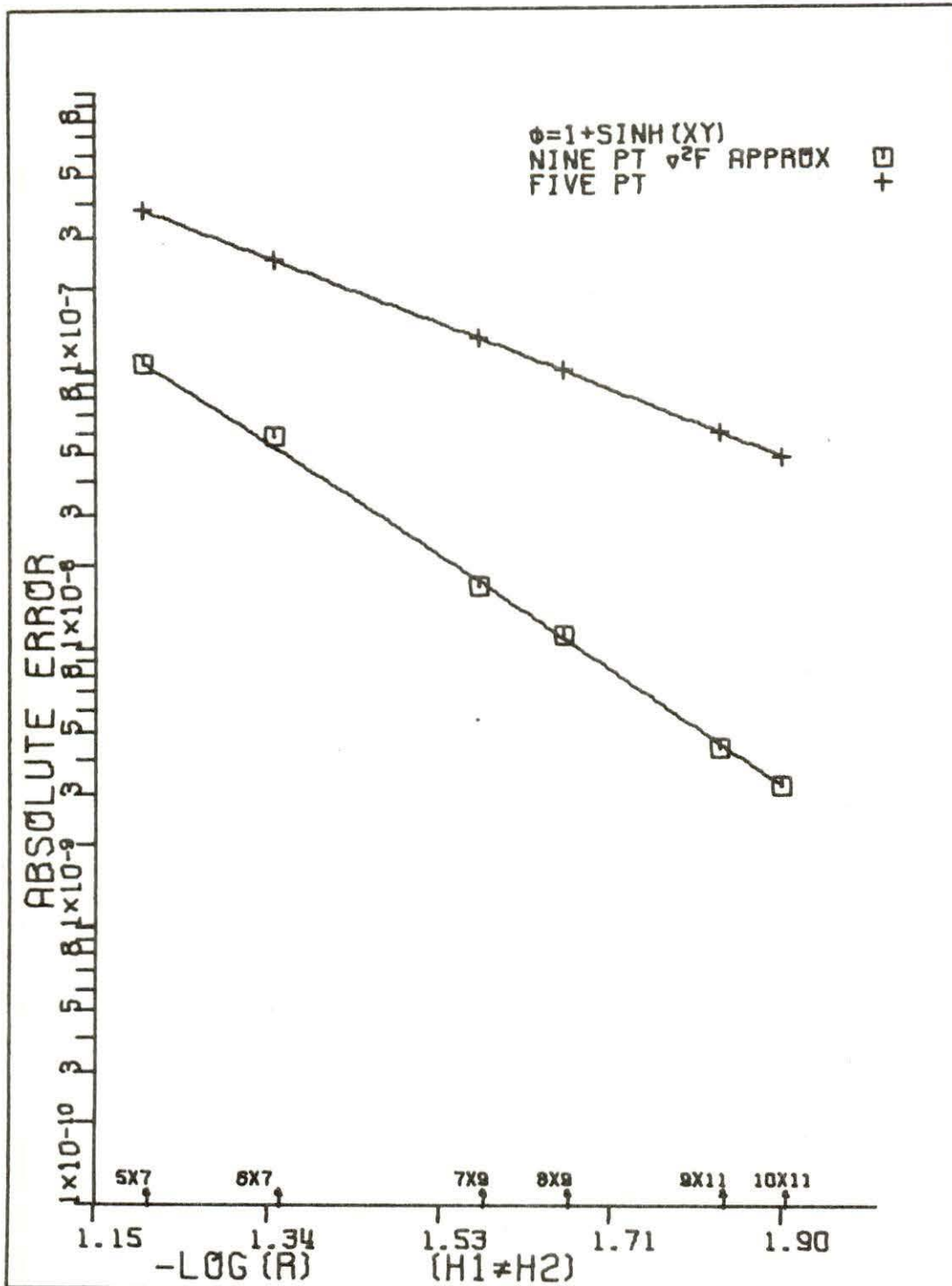


Fig. 14. Plot of absolute error as a function of R , where $R = \sqrt{h_1^2 + h_2^2}$, for $\phi = 1 + \sinh(xy)$ with x and y values ranging from -0.25 to 0.75 .

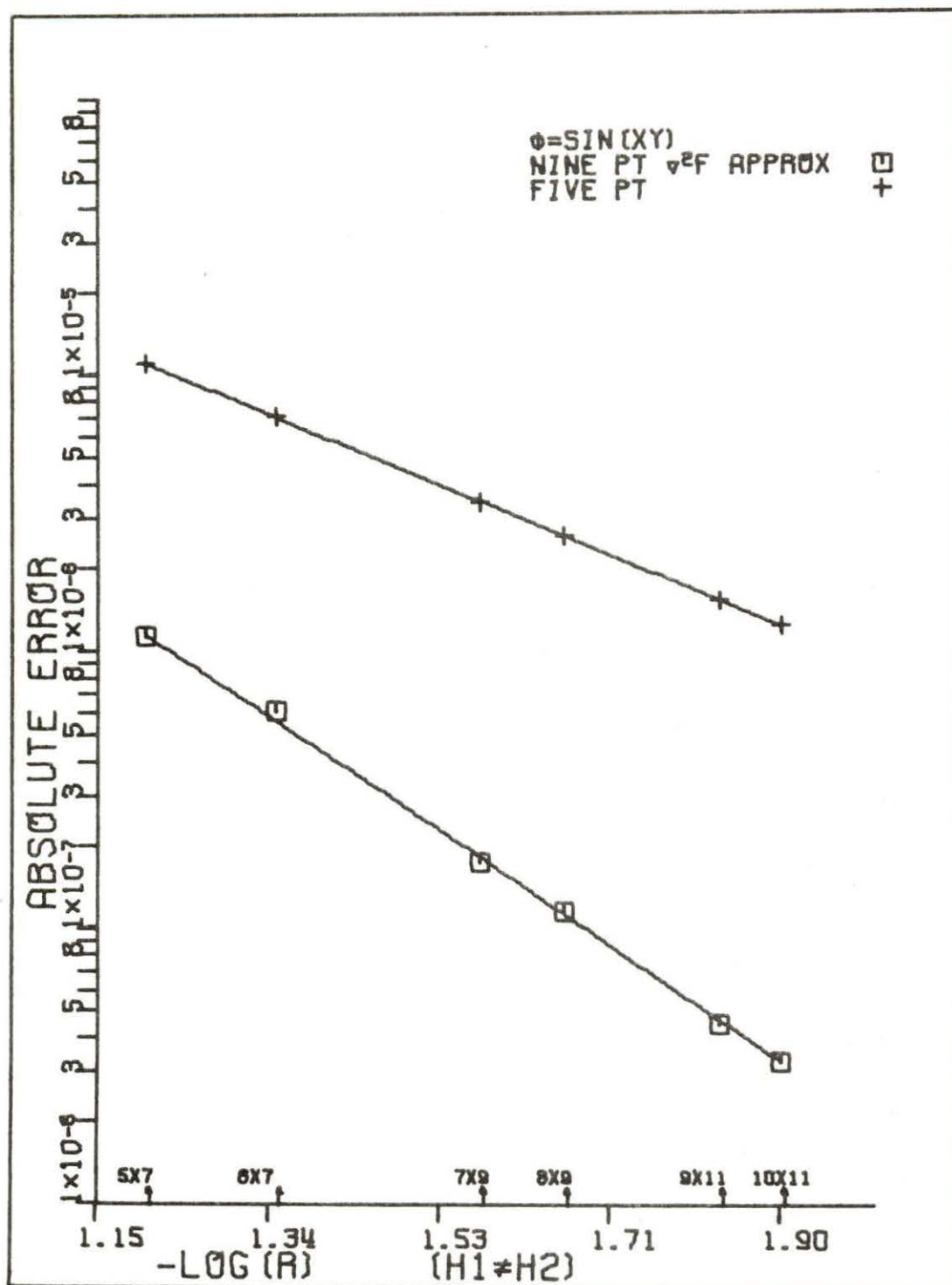


Fig. 15. Plot of absolute error as a function of R , where $R = \sqrt{h_1^2 + h_2^2}$, for $\phi = \sin(xy)$ with x and y values ranging from 0.1 to 1.1.

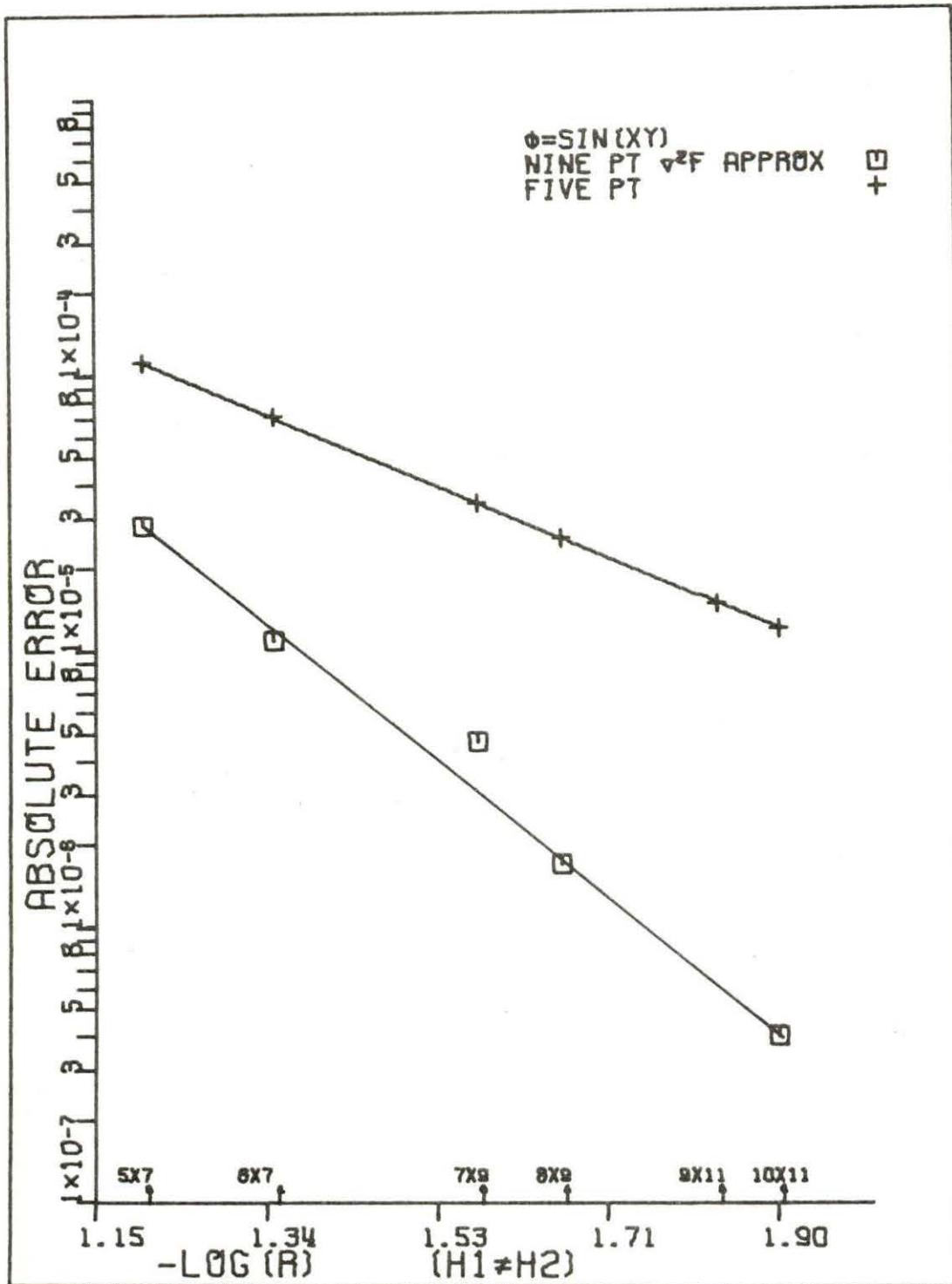


Fig. 16. Plot of absolute error as a function of R , where $R = \sqrt{h_1^2 + h_2^2}$, for $\phi = \sin(xy)$ with x and y values ranging from 0.5 to 1.5.

the curves resulting from the five- and nine-point calculations for a single case. In Figs. 10 and 11 the nine-point solutions are represented by two parallel lines. As indicated by the key in each figure, one line represents the case where the numerator of Eq. 2.15 was calculated analytically ($\nabla^2 f$ calc.). The other represents the case where the numerator is calculated using the numerical approximation given by Eq. 2.16 ($\nabla^2 f$ approx.). For the figures with only one line representing the nine-point solution, it is also indicated in the key which technique was used for evaluation of Eq. 2.15.

As can be seen in Figs. 10 and 11, the use of the numerical approximation of Eq. 2.16 for Eq. 2.15 led to some surprising results. The cases calculated using the approximation had consistently less error than the same problem calculated using the analytical value for the numerator of Eq. 2.15. It would seem that the error in the approximation for the numerator interacts in some manner with the error in the approximation of the denominator, Eq. 2.12, to produce a more accurate value for the parameter p . Thus the use of the approximation for the numerator not only simplified the application of the technique as described in Chapter 2, but it also produced a more accurate solution.

All but one of the cases considered gave similar results when plotted in the above described manner. The exception was the sine function applied to equally spaced regions with x and y values of 0.5 to 1.5. As can be seen in Fig. 13, the case produced two curves representing the nine-point solutions. Unlike the plots just discussed, these two curves represent calculations made using odd and even

numbers of grid points. For this particular case, the nine-point relation applied to a region with an even number of interior grid points gave an error value larger than the value achieved using an odd number of points. That is, the use of an odd number of interior grid points gave more accurate solutions than the use of an even number of points.

This discontinuity was not found for any other configuration of the sine function. Applying the same x and y values to unequal spacing did not give similar results, see Fig. 16. When x and y values of 0.1 to 1.1 were used with equal spacing, again there was no differential between odd and even numbers of points. The numerical approximation to the numerator of Eq. 2.15 was also applied to the original problem. It had no effect on the odd-even discontinuity other than lowering both curves a slight amount. The discontinuity in the error calculations was not the only problem encountered with this configuration of the sine function. A related phenomena was found in attempts at α optimization. This will be discussed in Section 4.4.

No adequate explanation for either phenomena has been determined. The discontinuities may stem simply from a peculiarity in the numerical values of the error derivative terms caused by those combinations of points. An explanation may come from the fact that when Eq. 2.15 is substituted for p in the nine-point relation, the resulting relation is nonlinear. Further work is needed to fully explain the discontinuities.

As mentioned previously the error analysis was completed only for the sine and hyperbolic functions. Attempts were also made to

analyze the error for two polynomials $x^2 + y^2 - 2x^2y^2$ and $x^4 + y^2 - 2x^3y^2$. The highest power in either equation was of order 4. As is seen in Eq. 2.6 the lowest derivative in the truncation error terms is of order 6. Thus when the polynomials were applied using the nine-point relation the truncation error derivative terms went to zero and therefore so did the truncation error. This meant that the nine-point relation applied to these polynomials had in essence no error.

The error in the final numerical solution was thus limited only by the accuracy of the computing system used. This meant that accurate error analysis could not be made for these polynomials. For accurate analysis to be made, polynomials of powers of order six or higher would have to be used. However because of time limitations, and the feeling that the sine and hyperbolic functions represented more common solutions, no further work with polynomials was attempted.

For all the error calculations that were completed, the relationships resulting between the logarithms of the absolute error and grid spacing were linear, as can be seen in Figs. 10 through 16. Because of this linear relationship it would be expected that the truncation error could be expressed as a function of grid spacing h by a relation of the form

$$\log e = n \log (h) + \log (c) \quad (4.1)$$

Such a relation would then result in the truncation error being represented by

$$e = c(h^n) \quad (4.2)$$

where n is the order of the truncation error, either 2 or 4 for the finite difference relations handled in this study, and where the coefficient c would contain the derivative terms of the truncation error. Thus it could be expected that the straight lines in the absolute error vs h plots would have a slope of either 2 for the five-point results or 4 for the nine-point results.

However the results of this study and the results of the study done by Holmes and Ettles [11] indicate that such is not the case. Both studies have found the slope of the lines to be noninteger values slightly larger than the expected values of 2 or 4. Holmes and Ettles have attempted to explain these results through the use of a relation of the form

$$\log e = m \log (h^n) + \log c \quad (4.3)$$

which results in the error being represented by

$$e = c (h^n)^m \quad (4.4)$$

The exponent n is once again either 2 or 4, and c still represents the truncation error derivative terms. The exponent m is used to account for the unexpected slope of the error vs h lines. Holmes and Ettles got values for m which range from 0.95 to 1.09. These values for m multiplied by the appropriate value of n then gave the slopes of the lines. The values for m found in this study were slightly larger. They are shown in Table 1 along with the appropriate values of the coefficient c , which seems to be significant in quantifying

Table 1. The parameters c and m for the absolute error vs grid spacing curves shown in Figs. 10 through 16

Function (x-y range)	Five point		Method for calc. $\nabla^2 f$	Nine point	
	c	m		c	m
1 + sinh (xy) (0.0 to 1.0)	6.55(10 ⁻⁴)	1.552	Analytical	6.98(10 ⁻³)	1.329
			Approximate	3.81(10 ⁻³)	1.338
1 + sinh (xy) (- 0.25 to 0.75)	4.59(10 ⁻⁵)	1.528	Analytical	8.78(10 ⁻⁴)	1.316
			Approximate	5.14(10 ⁻⁴)	1.331
1 + sinh (xy) (- 0.25 to 0.75) (unequal spacing)	1.30(10 ⁻⁵)	1.475	Approximate	4.57(10 ⁻⁵)	1.29
sin (xy) (0.1 to 1.1)	1.52(10 ⁻³)	1.585	Approximate	5.84(10 ⁻³)	1.341
sin (xy) (0.5 to 1.5)	1.87(10 ⁻²)	1.64	Analytical (odd)	2.39(10 ⁻²)	1.238
			Analytical (even)	1.001(10 ⁻¹)	1.183
sin (xy) (0.1 to 1.1) (unequal spacing)	4.83(10 ⁻⁴)	1.574	Approximate	5.11(10 ⁻⁴)	1.27
sin (xy) (0.5 to 1.5) (unequal spacing)	4.64(10 ⁻³)	1.552	Approximate	4.34(10 ⁻²)	1.52

the error. The results for calculations with unequal spacing are given in Table 1 as a function of R .

Holmes and Ettles offered no explanation as to the source of the exponent m . One possible explanation is to assume that m takes the form

$$m = 1 + \Delta \quad (4.5)$$

where Δ is some fractional value less than unity. With this assumption for m , Eq. 4.3 can be rewritten as

$$\log e = \log c' + (1 + \Delta) \log (h^n) \quad (4.6)$$

or

$$\log e = \log c' + \Delta \log (h^n) + \log (h^n) \quad (4.7)$$

By comparison of Eq. 4.7 with Eq. 4.1, it can be seen that the log of c from Eq. 4.1 can be described by

$$\log c = \log c' + \Delta \log (h^n) \quad (4.8)$$

This result would indicate that the coefficient c should have the form

$$c = c' (h^{\Delta n}) \quad (4.9)$$

If this analysis is accurate then one could expect the coefficient c and therefore the truncation error derivative terms to be functions of the grid spacing h . The exponent m thus may stem from some variation of the truncation error derivative terms with h .

A possible explanation for this variation may lie in the fact that as the grid spacing h is varied, the derivative terms are calculated at slightly different grid points giving slightly different values, and thus varying with h . A proof of this explanation has not been determined, however it can be shown to be true at least empirically. Suppose a point could be found where the x and y values did not vary with the grid spacing. The truncation error derivative terms at such a point would be constant for all values of h . Then if the above

explanation for m is to be true the error at that point calculated for several values of h should produce curves with slopes of 2 or 4.

It was found that for an equally spaced region with an odd number of points on each side the x and y values at the center point do not vary with the grid spacing. Several calculations were made using regions with such grids. The absolute error at the center point was calculated for each region. The resulting error values were then plotted versus h as before, see Fig. 17. The slope of the resulting nine-point curve was 4.0037 overall. The five-point curve was not linear at least for the grid spacing values used. Instead the slope of the curve successively increased for increased numbers of points. The slope increased from 1.61, between regions of 5×5 and 7×7 , to 1.93, between regions of 11×11 and 13×13 . Thus it would seem that the slope would approach 2 if larger regions were applied.

These results show that the curves, resulting from the error calculations at points where the derivatives do not vary, have the expected slopes of 2 and 4. This would seem to prove the above proposed explanation for the source of m , that is, the exponent m arises from the dependence of the truncation error derivative terms on the grid spacing h .

The values of the slope and coefficient c for the five- and nine-point curves are the key to showing the computational advantage of the nine-point relation. As stated in Section 4.1 this advantage was to be demonstrated by showing that the accuracy of the five-point solution to a problem could be achieved using the nine-point relation applied with many fewer points. This can now be done using Figs. 10 through 16

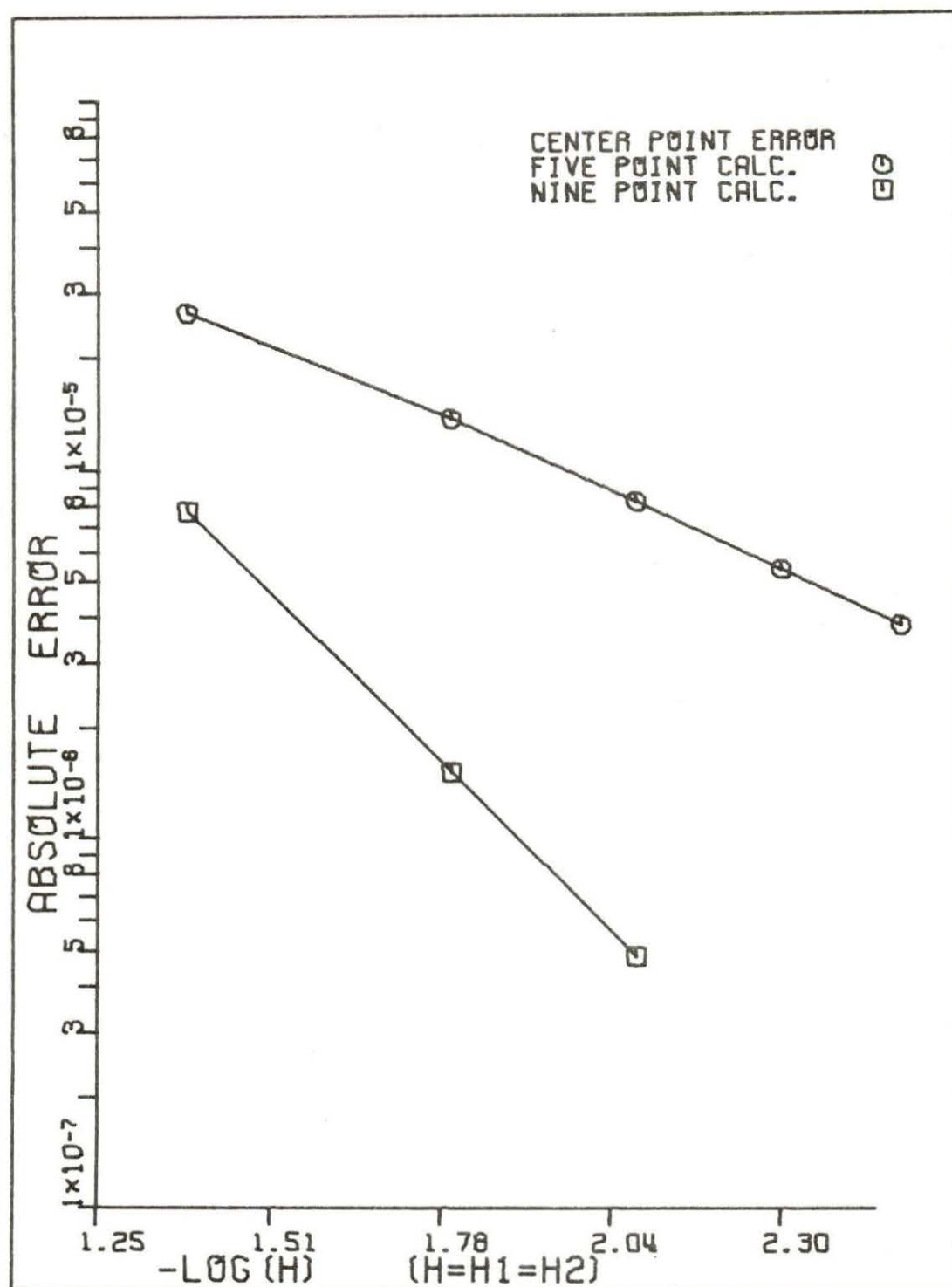


Fig. 17. Plot of absolute error vs h for the center point of a region with an odd number of points.

and the values of the slopes and coefficients c resulting from the curves in those figures.

If Figs. 10 through 16 are used, the analysis can be made easily. The value of error desired is located on the ordinate. Then by drawing a horizontal line from this point through both the five- and nine-point curves the corresponding values of h can be read from the abscissa directly below the respective intersection of the line and curve. These values for h can then be directly transformed into estimates for the number of points required for the desired error.

This direct use of the plots while simple can sometimes be inaccurate due to the difficulty in reading the values from the plots. The linearity of the curves allows for a more accurate method of analysis which involves the use of Eq. 4.4 and the slopes and coefficients c calculated from the original data. If Eq. 4.4 is rewritten as

$$h = mn\sqrt{\frac{e}{c}} \quad (4.10)$$

then the proper values of m , n and c from Table 1 can be used to calculate h for any error value chosen.

The later technique was used to calculate the results shown in Tables 2 and 3, in which the spacing and number of points required for equivalent error in the five- and nine-point solutions are shown. In Table 2 the results of two calculations are shown for each problem handled. In the first calculation the value of error calculated for the nine-point solution of the 12×12 region is used to calculate the equivalent spacing and number of points required by the five-point

Table 2. The spacing and number of points required for equivalent error in the five- and nine-point solutions to given configurations

Configuration	Error desired	Five-point grid			Curve used	Nine-point grid			F ^b
		h	Dimensions	Points ^a		h	Dimensions	Points ^a	
1 + sinh (xy) (0.0 to 1.0)	1.015(10 ⁻⁸)	0.0282	35 x 35	1089	Approx.	0.091	12 x 12	100	10.89
	4.148(10 ⁻¹⁰)	0.01	100 x 100	9604	Approx.	0.05	20 x 20	324	29.64
1 + sinh (xy) (-0.25 to 0.75)	1.4673(10 ⁻⁹)	0.0319	31 x 31	841	Approx.	0.091	12 x 12	100	8.41
	6.085(10 ⁻¹¹)	0.0106	94 x 94	8464	Approx.	0.05	20 x 20	324	26.1
sin (xy) (0.1 to 1.1)	1.5124(10 ⁻⁸)	0.0264	38 x 38	1296	Approx.	0.091	12 x 12	100	12.96
	6.133(10 ⁻¹⁰)	0.00961	104 x 104	10404	Approx.	0.05	20 x 20	324	32.11
sin (xy) (0.5 to 1.5)	1.7597(10 ⁻⁷)	0.0293	34 x 34	1024	Odd	0.1	11 x 11	81	12.64
	1.112(10 ⁻⁸)	0.0126	79 x 79	5929	Odd	0.0526	19 x 19	289	20.52

^aNumber of points which are calculated, that is, the number of interior points.

^bF = $\frac{\text{Number of points required by 5 pt.}}{\text{Number of points required by 9 pt.}}$

Table 3. The spacing and number of points required for equivalent error in the five- and nine-point solutions to give unequally spaced configurations

Configuration	Error desired	Five-point grid			Nine-point grid			F^c
		R	Dimensions ^a	Points ^b	R	Dimensions	Points ^b	
$1 + \sinh(xy)$ (-0.25 to 0.75)	$3.156(10^{-9})$	0.0595	22 x 22	484	0.1495	10 x 11	72	6.72
$\sin(xy)$ (0.1 to 1.1)	$3.2754(10^{-8})$	0.0474	28 x 28	784	0.1495	10 x 11	72	10.89
$\sin(xy)$ (0.5 to 1.5)	$4.0223(10^{-7})$	0.0491	27 x 27	729	0.1495	10 x 11	72	10.125

^aDimensions of equally spaced region required for given R value.

^bNumber of points which are calculated, that is, the number of interior points.

^c $F = \frac{\text{Number of points required by 5 pt.}}{\text{Number of points required by 9 pt.}}$

relation for the same error. In the second calculation, the error in the nine-point solution for a 20 x 20 region was calculated using Eq. 4.4 and data from Table 1. Then this value for the error was used to estimate the spacing and number of points required for the five-point relation for the same error. For all cases handled with unequal spacing only one calculation was made, see Table 3. In this calculation the value of error calculated for the nine-point solution for the 10 x 11 region was used to calculate the equivalent value of R required by the five-point relation.

The dimensions and therefore the number of points are listed in Table 2. For cases where they were not originally known, estimates were made by rounding the exact values for the dimensions calculated from h to integer values. The number of points listed in Table 3 were estimated by assuming that the calculated values of R represent equally spaced grids. Then R could be represented by $\sqrt{2}h$ from which h and values for the number of points could be estimated. The number of points listed in both tables is the number of points that would be calculated in the region.

From the calculations shown in Table 2, it can be seen that the computational advantage expected was obtained by using the nine-point relation. The values of the ratio F emphasizes the magnitude of this advantage. In order to achieve the error realized by a nine-point calculation using an equally spaced 12 x 12 region, a five-point calculation would require anywhere from 8 to 13 times as many points. Even more important, as the regions become larger the savings become even more pronounced. To achieve the error in an equally spaced 20 x 20

nine-point calculation, from 26 to 32 times more points would need to be used by the five-point relation. The results shown in Table 3 indicate that similar savings can also be expected for problems using unequal spacing.

4.3 Convergence Analysis

The savings in the number of grid points previously shown for the nine-point relation clearly indicates a reduction in the computer storage required. This advantage however may be of little value if the nine-point solution converges at a slower rate than the five-point solution for equivalent error. The savings in storage cost could easily be outweighed by increased cost for computation time. Thus in order to show the computational advantage of using the nine-point relation an analysis of the relative speeds of convergence for the five- and nine-point relations was required.

It would seem that the speed of convergence could be compared easily through the use of the number of iterations or convergence rate ν . However it must be remembered that each technique will require a different number of calculations and therefore a different amount of time for each iteration. Thus to make any comparison of speed of convergence both the time required per iteration and the total number of iterations necessary for convergence must be considered. That is, the actual computing time for convergence of each technique must be compared.

A method for estimating the total computational time was developed for this study. It involved the estimation of the time required per grid point for the calculation of one iteration. The computation time expressed in such a manner was used because it was independent of the number of grid points used for the region. This time estimate was made by breaking the computer program into three separate sections, the main program, the five-point subroutine and the nine-point subroutine. A sample problem was then applied to each section and from these calculations the central processor (CPU) times for the respective five- and nine-point calculations were found. Then using the number of iterations to convergence and the number of grid points calculated for the sample problem a value for the time per point per iteration was calculated for both the five- and nine-point calculations. Now the total computation time for the sample problem applied with any other number of grid points could be calculated. The computation time could be found by multiplying the product of P (number of grid points) times I (number of iterations to convergence) for the new problem by the constant value of time per point per iteration.

The above method was well adapted for estimating the computation time for configurations applied in this study. Just by calculating the $P \cdot I$ value for the solution of any problem an estimate could be made for the computation time required to achieve that solution. However the comparison of the five- and nine-point solutions for equal error values resulted in regions being discussed which had larger grids than any which were applied in this study. This led to the problem of how to estimate the computation time for regions with grids

which had not been applied, and for which P-I values could not be directly calculated. Further development of the above method was required for such cases.

For a particular configuration applied, the values of P-I could be calculated for each set of grid points used with the configuration. The resulting values of P-I could be plotted logarithmically as a function of the respective grid spacing h . The plots resulting from such calculations were nearly linear. These curves could therefore be extrapolated, at least approximately, to give estimates for P-I values corresponding to any grid spacing. Thus from such plots, estimates for P-I values and therefore computation times could be made for the original configuration with any number of grid points.

Because estimates for the computation time could now be made for any number of grid points used, the results from Section 4.2 could now be evaluated with respect to the computation time. That is, the computation time required by the five- and nine-point solutions for equal error could now be estimated.

At this point the accuracy of using the actual number of iterations to convergence as a measure of speed of convergence should be discussed. As mentioned in Section 3.3 the actual number of iterations to convergence can be an inaccurate measure of the speed of convergence. The inaccuracy can be caused by the initial conditions for the iteration vectors. Initially the iterated vector depends upon all of the eigenvalues and eigenvectors of the iteration matrix [9]. However the smaller eigenvalues eventually decay and the

largest eigenvalue λ_1 is asymptotically approached. Once λ_1 is reached the solution converges at a constant rate, this constant rate of convergence has been previously defined as the convergence rate ν .

As defined in Section 3.3 the convergence rate ν is equal to the negative log of λ_1 . This means that ν is in effect a measurement of the speed of convergence independent of the effect of the smaller eigenvalues and therefore also the initial conditions of the iteration matrix. The use of the convergence rate ν would thus be a more objective measure of speed of convergence for comparison purposes. If the actual number of iterations were used in a comparison, the initial conditions could affect the objectivity of the study. The relative speeds of convergence could be varied simply through the use of the proper initial conditions. *not generally true*

As just stated, the convergence rate ν would be excellent for comparison purposes, but the time comparison analysis just described was developed to use a value for the number of iterations. An estimate for the number of iterations corresponding to ν and therefore independent of the initial conditions was necessary for an objective time analysis to be made.

In Section 3.3 the convergence rate ν was defined also as being equal to the slope of the residual error norm versus iteration curve. However in actual practice the slope of these curves only approaches ν after the smaller eigenvalues have decayed. Thus in the definition of ν it is assumed that the slope of the entire curve is constant and equal to ν and is therefore assumed independent of the initial conditions.

This assumption meant that the convergence rate could be described by the relation

$$\nu = \frac{\ln \|r_2\| - \ln \|r_1\|}{\text{iter}_2 - \text{iter}_1} \quad (4.11)$$

This relation can be rearranged to give

$$\text{iter}_2 - \text{iter}_1 = \frac{\ln \|r_2\| - \ln \|r_1\|}{\nu} \quad (4.12)$$

Equation 4.12 could be used to estimate a value for the total number of iterations which is independent of the starting conditions. For the cases analyzed in this study the number of iterations was calculated from Eq. 4.12 in the form

$$\text{total number of iterations} = \frac{-\ln(10^{-10})}{\nu} \quad (4.13)$$

The computation time analysis was only completely applied to one configuration, $\phi = 1 + \sinh(xy)$ with x and y values ranging from - 0.25 to 0.75 and with the numerator of Eq. 2.15 approximated. This configuration was applied with a 12 x 12 equally spaced region for the initial time per point per iteration calculations. The results of these calculations are shown in Table 4. From the results in Table 4 it can be seen that the nine-point relation takes over twice as long for computation per point per iteration, as would be expected.

The application of the above configuration to the error analysis of Section 4.2 resulted in the five- and nine-point relations being applied to eight error calculations. The convergence rate ν from each of the five- and nine-point solutions was used with Eq. 4.13

Table 4. Results of time per point per iteration calculations

Section of program	Time/calc. (sec.)	Points calculated	Iterations ^a	t/P·I ^b (sec.)
Five-point subroutine	2.07	100	184	1.125(10 ⁻⁴)
Nine-point subroutine	4.62	100	175	2.64(10 ⁻⁴)

^aThe actual number of iterations to convergence.

^bt/P·I = time per point per iteration.

to calculate the number of iterations for each solution. These iteration values were then used with the number of grid points to calculate P·I values corresponding to the respective five- and nine-point solutions. These calculations resulted in eight P·I values for each technique, corresponding to each of the eight h values. The results are shown in Table 5. The results of the five-point P·I calculations were used to formulate a P·I versus h plot as previously described, it is shown in Fig. 18.

As can be seen in Fig. 18, the curve resulting from the P·I versus h plot for the five-point calculations is nearly linear. Because of this linearity the line could be extrapolated and values of P·I could be estimated for values of h not applied in this study. This capability was used to make an error versus time analysis for the results of Section 4.2. Shown in the first column of Table 6 are the error values resulting from the eight nine-point solutions calculated for the $1 + \sinh(xy)$ configuration.

Table 5. Results of P-I calculations for five- and nine-point solutions to $1 + \sinh(xy)$

Region	h	Points calc.	Five-point results			Nine-point results		
			ν	Iter. ^a	P·I	ν	Iter. ^a	P·I
5 x 5	0.25	9	1.2685	18	162	1.2264	19	171
6 x 6	0.2	16	0.64908	36	576	0.62836	37	592
7 x 7	0.167	25	0.41906	55	1375	0.40954	56	1400
8 x 8	0.143	36	0.29671	78	2808	0.29169	79	2844
9 x 9	0.125	49	0.22224	104	5096	0.23076	100	4900
10 x 10	0.111	64	0.17311	133	8512	0.1713	135	8640
11 x 11	0.1	81	0.13885	166	13446	0.13766	167	13527
12 x 12	0.091	100	0.11394	202	20200	0.11312	204	20400

^aIterations calculated from $\frac{-\ln(10^{-10})}{\nu}$ and rounded to nearest integer value.

For each of these error values the corresponding five-point grid spacings required to give each specified error was calculated using Eq. 4.4 with data from Table 1. These h values were then used with the plot in Fig. 18 to estimate P-I values corresponding to each value. The P-I estimates were then multiplied by the time per point per iteration to give the approximate time required by a five-point solution for the specified error. The computation times for the corresponding nine-point solutions were calculated directly from the already known P-I values. The results of these computation time calculations are shown in Table 6. The resulting five- and nine-point

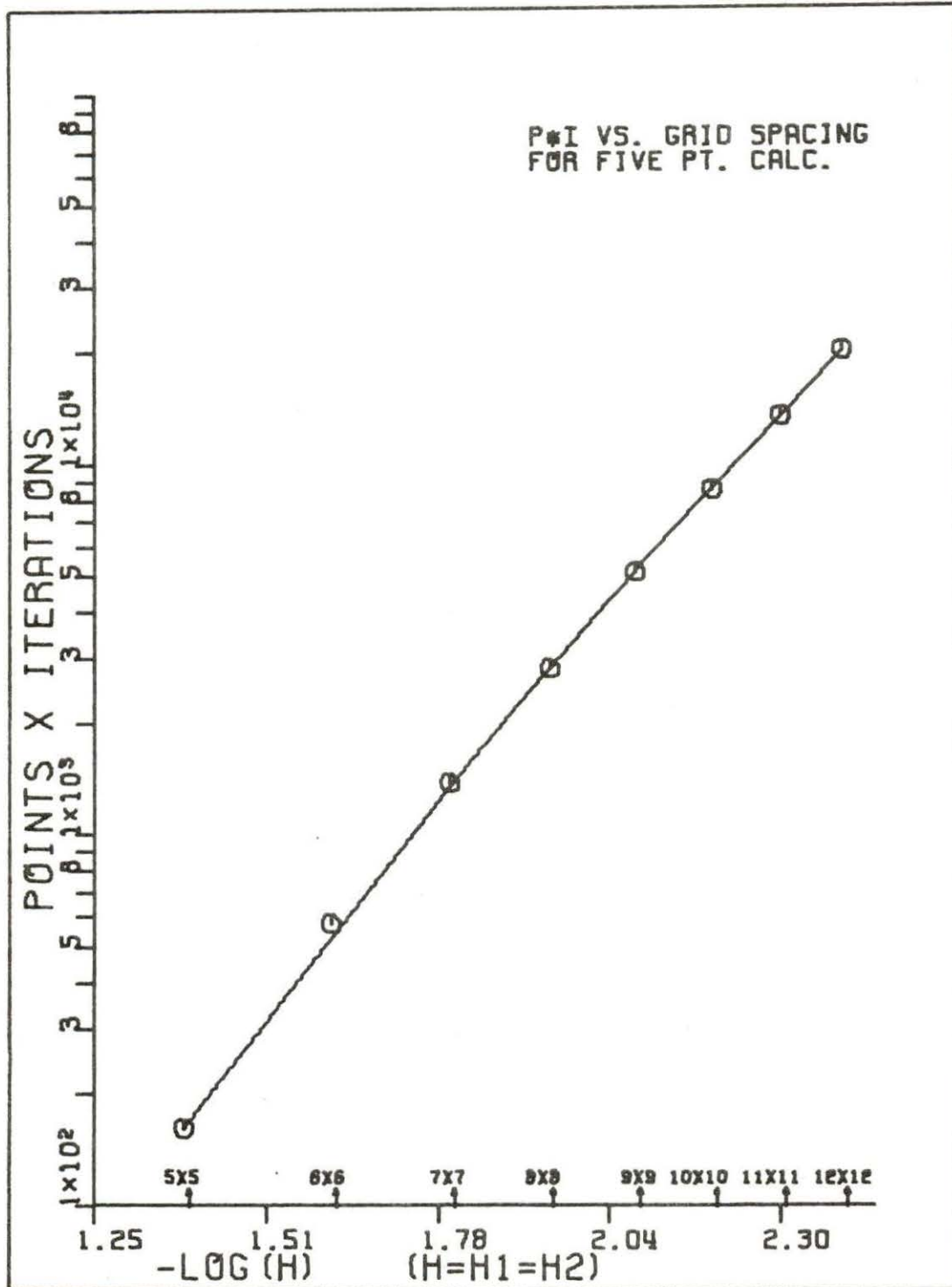


Fig. 18. Plot of the product of P (number of points) times I (number of iterations to convergence) as a function of the grid spacing h for five-point calculations using $1 + \sinh(xy)$.

Table 6. Results of error versus time analysis for $1 + \sinh(xy)$ with x and y values ranging from -0.25 to 0.75

Nine-point error	Five-point results			Nine-point results			G^a
	h	P.I	Time (sec.)	h	P.I	Time (sec.)	
$3.203(10^{-7})$	0.206	540	0.064	0.25	171	0.045	1.4
$9.4967(10^{-8})$	0.135	3400	0.38	0.2	592	0.16	2.4
$3.5607(10^{-8})$	0.0963	16000	1.8	0.167	1400	0.37	4.9
$1.5654(10^{-8})$	0.0724	55000	6.2	0.143	2844	0.75	8.3
$7.726(10^{-9})$	0.0567	167000	18.8	0.125	4900	1.29	14.5
$4.1688(10^{-9})$	0.0458	430000	48.4	0.111	8640	2.28	21.2
$2.4055(10^{-9})$	0.0379	990000	111.4	0.1	13527	3.57	31.2
$1.4673(10^{-9})$	0.0319	2190000	246.4	0.091	20400	5.38	45.8

$$a_G = \frac{\text{Computation time} - 5 \text{ pt.}}{\text{Computation time} - 9 \text{ pt.}}$$

computation times were also plotted logarithmically as a function of the corresponding error. This plot is shown in Fig. 19.

From the results shown in Table 6 and Fig. 19 it can be seen that a definite savings in computation time is gained by the use of the nine-point relation. The values of the ratio G in Table 6 indicate that a five-point solution with the error of a 5×5 nine-point solution would require almost 1.5 times more computation time than the nine-point solution. To achieve the error in a 12×12 nine-point solution the five-point solution would require nearly 46 times more computation time. It can now be seen from Tables 2 and 6, that for the five-point relation to give the same error as the 12×12

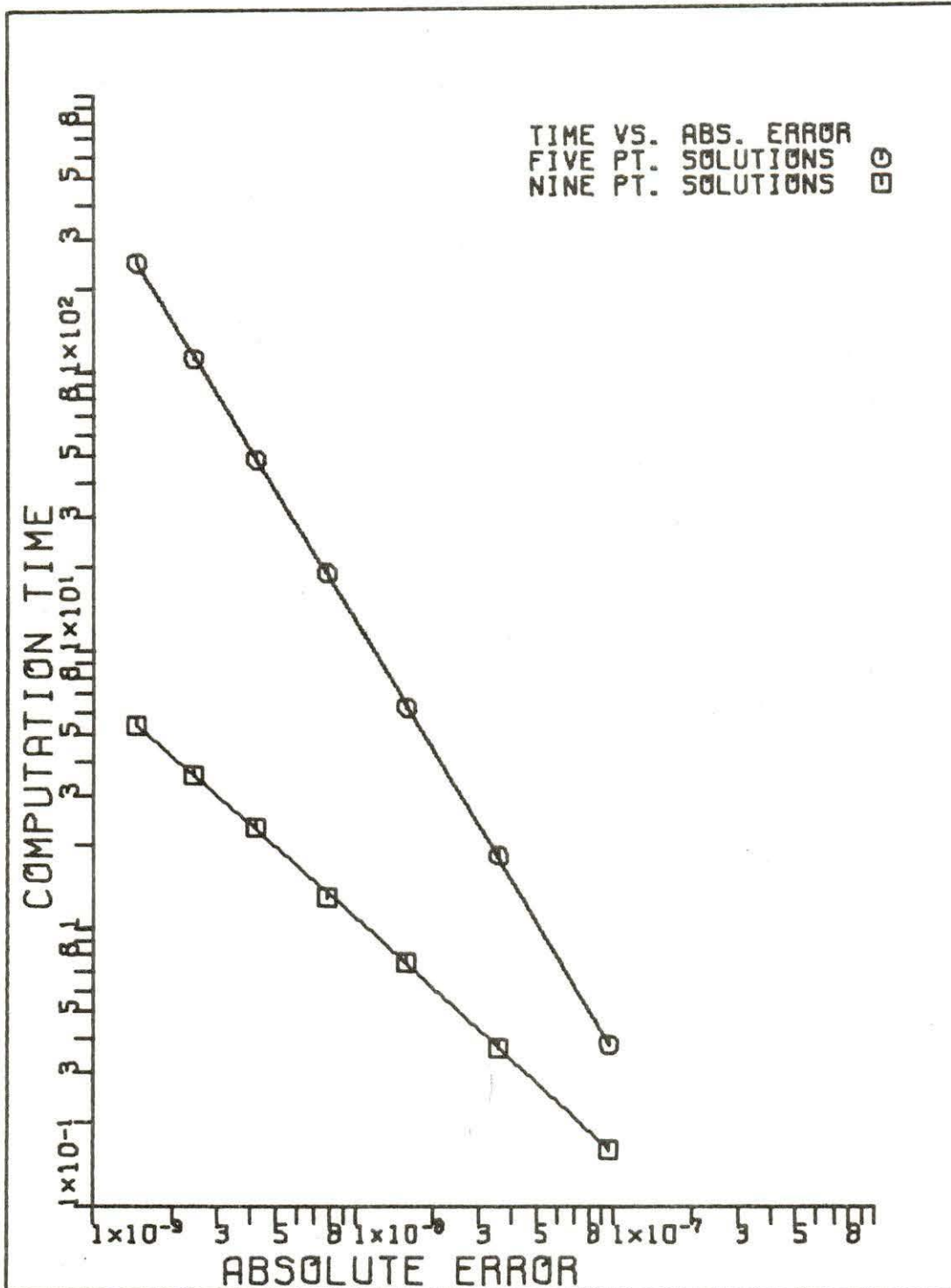


Fig. 19. Plot of the computation time in seconds as a function of the absolute error for five- and nine-point calculations using $1 + \sinh(xy)$.

nine-point solution 8 times more points and over 45 times more computation time would be required. These results show a large computational advantage for the use of the nine-point relation, an advantage which increases with the accuracy required.

At this point it must be remembered that the five-point computation time figures just used are only approximate. The extrapolation of the P·I versus h plot was only approximate and the P·I values resulting from the extrapolation are therefore subject to some inaccuracy. The figures were presented for comparison purposes only and are accurate enough to show at least qualitatively that for equivalent error the nine-point relation will take much less computation time.

4.4 Optimization of the SOR Technique

As mentioned earlier the majority of the calculations in this study were made without attempting to optimize the SOR technique. The calculations used for the computation time analysis just discussed were made using a constant value of $\alpha = 1.15$ for both the five- and nine-point solutions. As can be seen in Table 5 this resulted in values for the convergence rate ν which were nearly equivalent for the five- and nine-point solutions. The question which arises at this point is what happens when α_{opt} is used for the five- and nine-point solutions. Will the use of α_{opt} greatly affect the relative computation times of the five- and nine-point relations?

As discussed in Section 4.2 optimization was attempted only for the function $\sin(xy)$ applied with x and y values ranging from 0.5 to

1.5. Attempts were made to optimize the $\sin(xy)$ configuration applied to four equally spaced grids ranging from 5×5 to 8×8 . A largely trial and error process was used for the optimization attempt. Only λ_1 versus α plots, as described in Section 3.3, were used to aid the process.

As was shown in Section 4.2 this configuration of the sine function has very pronounced discontinuities in the error analysis results. These discontinuities were carried into the optimization process. As with the error calculations for this configuration, a discontinuity between regions with odd and even numbers of grid points was found when attempts were made to optimize the nine-point relation. These discontinuities made it impossible to use this configuration to answer any question with respect to the effect of α_{opt} .

When the nine-point relation was applied to regions with an odd number of grid points, the λ_1 versus α curves which resulted were very similar to the expected curves from five-point calculations. An example of the plots resulting from the nine-point relation optimization is shown in Fig. 20 for the 5×5 region. The nine-point relation applied to regions with an even number of grid points resulted in plots that were very much different from the expected curves. As can be seen in Fig. 21, for the 8×8 region the slope of the λ_1 versus α curve increased very gradually up to what appeared to be α_{opt} where it reversed and gradually decreased.

The expected steep drop in the curve to the α_{opt} value for λ_1 was not present for either of the even grids used. The absence of this rapid drop resulted in a very slow convergence, even at α_{opt} , for both even grid regions. This slow convergence and the large

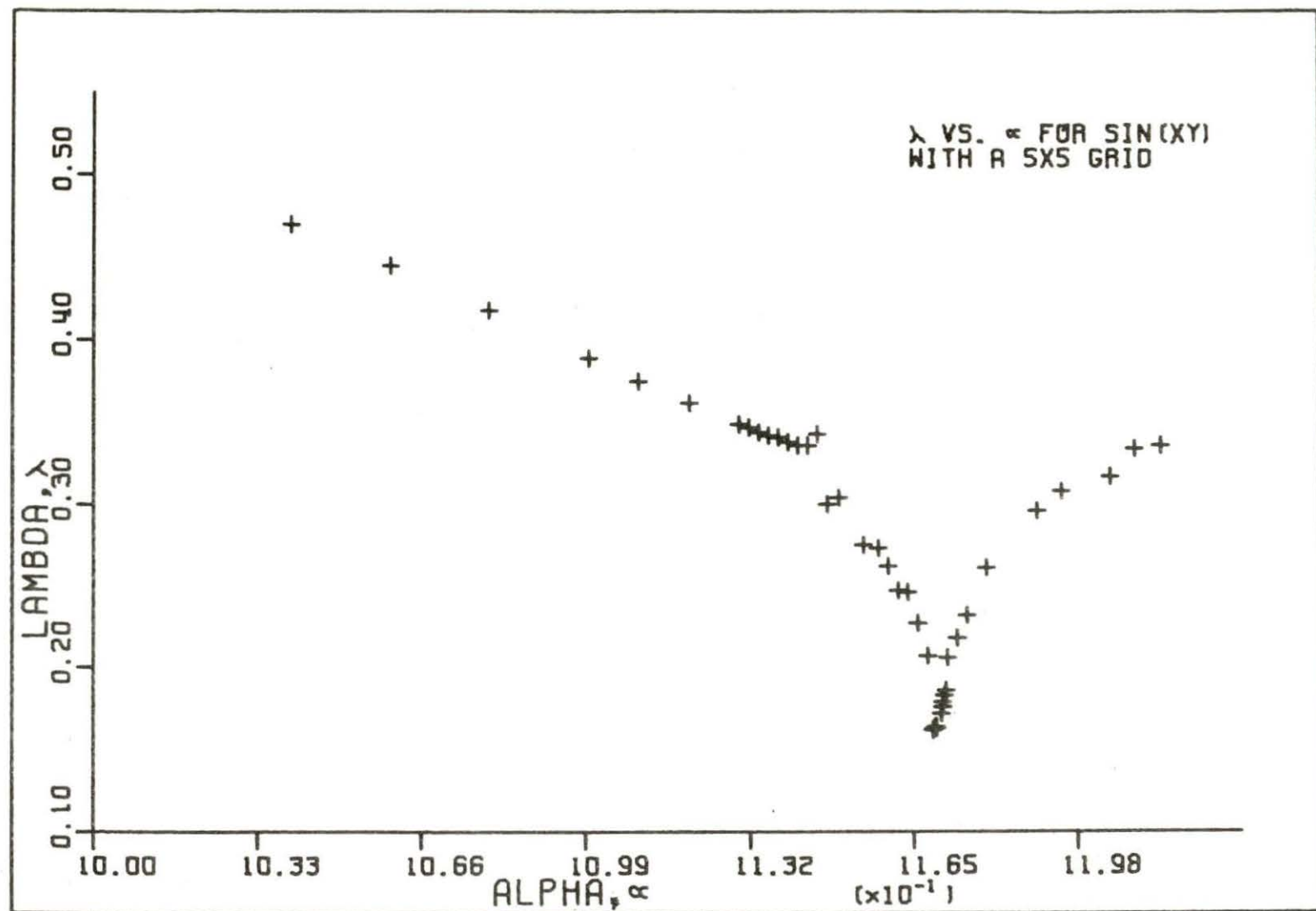


Fig. 20. Plot of the eigenvalue λ_1 as a function of the SOR parameter α for optimization calculations using the function $\sin(xy)$ with a 5×5 grid.

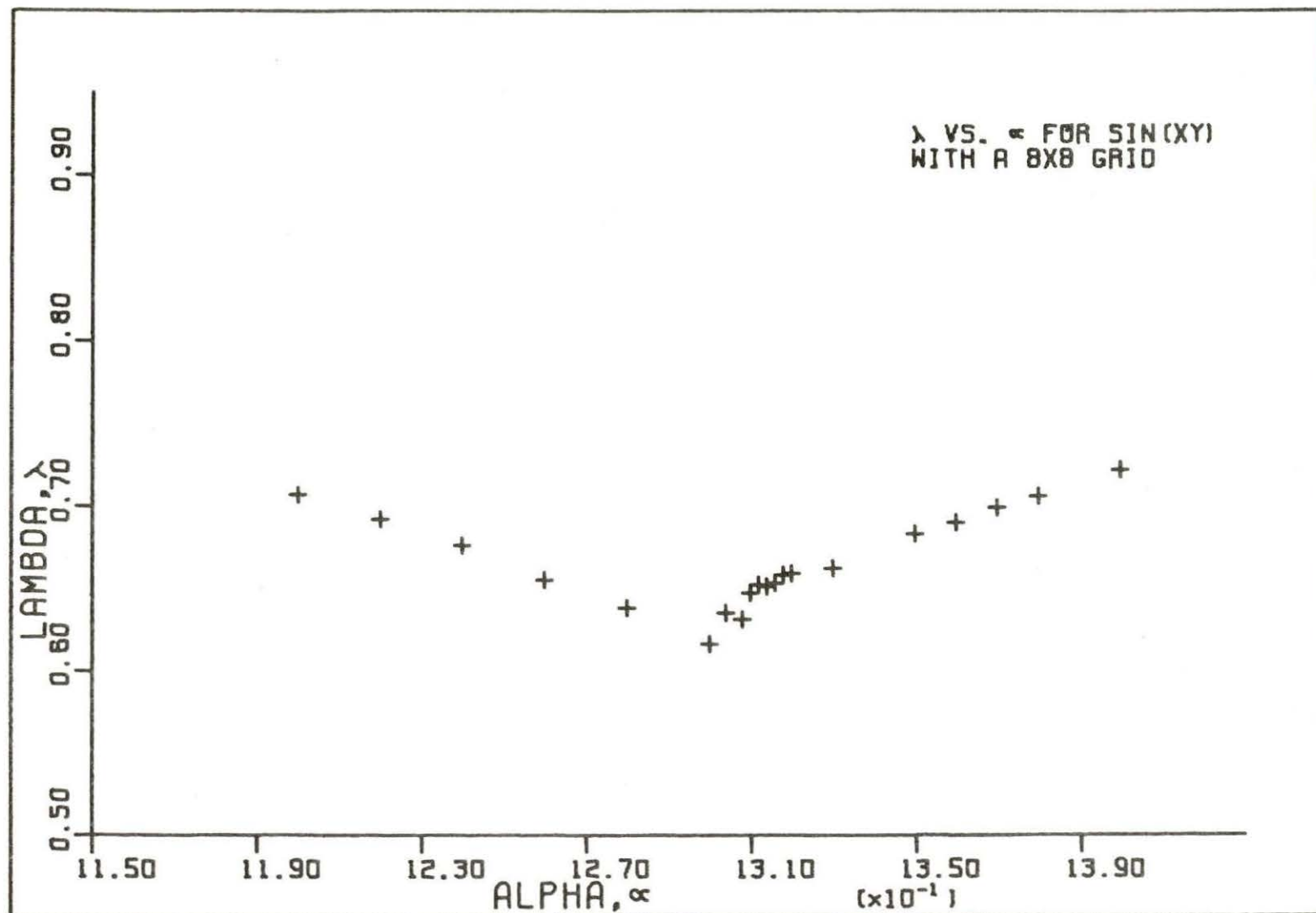


Fig. 21. Plot of the eigenvalue λ_1 as a function of the SOR parameter α for optimization calculations using the function $\sin(xy)$ with an 8×8 grid.

difference between the odd and even regions can be also seen from the values of ν shown in Table 7.

Table 7. Results of SOR optimization process for $\sin(xy)$

Region	<u>Five-point solutions</u>		<u>Nine-point solutions</u>	
	α_{opt}	ν	α_{opt}	ν
5 x 5	1.1748	3.01	1.169	1.82
6 x 6	1.2619	1.53	1.0943	0.597
7 x 7	1.3454	1.40	1.2840	1.25
8 x 8	1.4060	1.13	1.30	0.485

As stated previously no conclusive explanation has been found for these discontinuities. Also because of the discontinuities no conclusions on the effect of α_{opt} on the computation time analysis could be made.

CHAPTER 5. CONCLUSIONS

In this investigation it has been shown that the nine-point finite difference approximation to the two-dimensional Poisson's equation has higher accuracy than the usual five-point approximation. This higher accuracy was shown for several configurations. Included in these configurations were functions representing the three general types of differential equation solutions, that is, trigonometric, exponential or hyperbolic and polynomial. It was also found that the relative accuracy of the nine-point formulation increased with the number of points used. That is, the accuracy of the nine-point solutions increased more rapidly than the accuracy of the five-point solutions for decreasing grid spacing.

The use of the parameter p was shown to be an appropriate means for reducing the truncation error of the nine-point relation. The approximation used for the denominator of the equation describing p did not seem to adversely affect the overall error of the nine-point formulation. It was also found that the further approximation of the numerator of the same equation acted to reduce the overall truncation error as well as simplifying the application of the technique. Relatively few difficulties were found in applying the parameter p . Due to oscillations some configurations required either under- or over-relaxation of the SOR calculation of p to achieve convergence. Also it was found that care was necessary to avoid configurations where the cross derivative in the equation describing p went to zero.

It was discovered that the truncation error derivative terms were functions of the grid spacing h . Because of this dependence the overall truncation error norms were found to be a function of h to some non-integer power greater than the expected value of 4. The truncation error was of order 4 only at the points where the truncation error derivative terms were independent of h . Similar results were also found for the five-point solutions. Further it was shown that the truncation error for unequally spaced grids could be described using R , where $R = \sqrt{h_1^2 + h_2^2}$.

The λ_1 versus α curves resulting from the SOR optimization process for the nine-point relation were found to have the same shape as those resulting from the five-point relation. This indicates that because a value for α_{opt} could be found, the SOR technique should be useful in applying the nine-point relation. However not enough work was done to make any definite conclusions on the relative speed of the five- and nine-point relations at α_{opt} .

It was shown that the use of the nine-point relation provides very significant computational advantages. It was found that the accuracy of a five-point solution could be achieved using a nine-point relation with many fewer points. Further when applied in this manner the nine-point relation was found to require substantially less computation time. The combination of these findings indicate that large savings in both storage cost and computation time cost could be achieved by using the nine-point relation, while still providing more than adequate accuracy. Even more important, as more accuracy is required the relative savings from the nine-point relation increases.

CHAPTER 6. SUGGESTIONS FOR FURTHER STUDY

The following are suggestions for further investigation related to this work:

- 1) Further work is needed in the area of optimization of the SOR technique applied to the nine-point relation. The affect of using α_{opt} on the relative five- and nine-point convergence rates should be analyzed. An expression to predict the value of α_{opt} for the nine-point relation should be investigated. Also the affect on the convergence rate of the under- and over-relaxation of the SOR calculation of p should be examined.
- 2) An attempt should be made to explain the discontinuities in the sine function results. It should be determined whether the discontinuities were just a peculiarity for that configuration or whether similar discontinuities could occur for other configurations. Possible explanations may lie in the nonlinearity of the formulation resulting from the substitution of the equation for p into the nine-point relation or in some affect of the smaller eigenvalues of the iteration matrix.
- 3) The effects of applying the nine-point relation to configurations with larger and more rapidly varying functions could be investigated. Analysis of the nine-point relation with h values greater than unity may also be beneficial.
- 4) Configurations using irregularly shaped regions, such as in Fig. 8, could be analyzed with particular interest in the affect of the nine-point relation on calculations in corners and contractions.

5) Further studies could also be made using higher order polynomials, although the results of this study indicate that the nine-point relation applied to them would give results similar to those found already.

LITERATURE CITED

1. Bickley, W. G. 1948. Finite Difference Formulae for Square Lattice. *Quart. Mech. Appl. Math.* 1: 35-42.
2. Mikeladze, S. H. 1934. Sur l'integration numerique d'equations differentielles aux derivees partielles. *Bull. Acad. Sci. URSS* 6: 819-841.
3. Fox, L. 1962. Numerical Solutions to Ordinary and Partial Differential Equations. Pergamon Press, Inc., New York. 509 pp.
4. Greenspan, D. 1957. Note on Difference Equation Approximations of Laplace's Equation. *J. Franklin Institute* 268: 46-52.
5. Smith, G. D. 1965. Numerical Solution of Partial Differential Equations. Oxford University Press, New York. 175 pp.
6. Collatz, L. 1962. The Numerical Treatment of Differential Equations. 3rd ed. Springer-Verlag, Berlin. 568 pp.
7. Greenspan, D. 1959. On 'Best' Nine-Point Laplace Difference Analogues on Rectangular Grid. *Quart. Mech. Appl. Math.* 12: 111-116.
8. Young, D. 1954. Iterative Methods for Solving Partial Difference Equations of Elliptic Type. *Trans. Am. Math. Soc.* 76: 92-111.
9. Clark, J. M., and K. F. Hansen. 1964. Numerical Method of Reactor Analysis. Academic Press, New York. 340 pp.
10. Rohach, A. 1973. Application of a Nine-Point Relation to the Eigenvalue Problem. *Trans. Am. Nucl. Soc.* 17: 232-233.
11. Holmes, A. G., and C. M. M. Ettles. 1975. A Study of Iterative Solution Techniques for Elliptic Partial Differential Equations with Particular Reference to the Reynold's Equation. *Comp. Math. Appl. Mech. Engr.* 5: 309-328.
12. Wachspress, E. L. 1966. Iterative Solution of Elliptic Systems. Prentice-Hall, Inc., Englewood Cliffs, N.J. 299 pp.

ACKNOWLEDGMENTS

The author wishes to express his deepest gratitude to his major professor, Dr. Alfred Rohach, whose guidance and helpful contributions made this work possible. In addition, the author expresses appreciation to the Department of Chemical Engineering and Nuclear Engineering for its financial support, and to the Iowa State University Engineering Research Institute for providing funds for computer operations.

In conclusion, sincere gratitude is given to my wife, Jerri, for her help and encouragement throughout my graduate study.

APPENDIX A. DERIVATION OF FIVE-POINT FINITE DIFFERENCE

APPROXIMATION TO THE TWO-DIMENSIONAL POISSON EQUATION

The two-dimensional Poisson's equation in rectangular coordinates can be written as

$$\frac{\partial^2 \phi}{\partial x^2} + \frac{\partial^2 \phi}{\partial y^2} = \nabla^2 \phi = f(x, y) \quad (\text{A.1})$$

This relation can be approximated by a five-point finite difference equation. To relate the derivatives to the respective finite differences, use the Taylor's series expansion

$$\phi(x \pm h) = \phi(x) \pm h\phi'(x) + \frac{h^2}{2!} \phi''(x) \pm \frac{h^3}{3!} \phi'''(x) \pm \dots \quad (\text{A.2})$$

Using a finite difference grid as shown in Fig. 2, and expanding each of the four axial points about the center points results in

$$\phi_1 = \phi_0 + h_1 \frac{\partial \phi_0}{\partial x} + \frac{h_1^2}{2!} \frac{\partial^2 \phi_0}{\partial x^2} + \frac{h_1^3}{3!} \frac{\partial^3 \phi_0}{\partial x^3} + \dots$$

$$\phi_2 = \phi_0 + h_2 \frac{\partial \phi_0}{\partial x} + \frac{h_2^2}{2!} \frac{\partial^2 \phi_0}{\partial x^2} + \frac{h_2^3}{3!} \frac{\partial^3 \phi_0}{\partial x^3} + \dots$$

$$\phi_3 = \phi_0 - h_1 \frac{\partial \phi_0}{\partial y} + \frac{h_1^2}{2!} \frac{\partial^2 \phi_0}{\partial y^2} + \frac{h_1^3}{3!} \frac{\partial^3 \phi_0}{\partial y^3} + \dots$$

$$\phi_4 = \phi_0 - h_2 \frac{\partial \phi_0}{\partial y} + \frac{h_2^2}{2!} \frac{\partial^2 \phi_0}{\partial y^2} + \frac{h_2^3}{3!} \frac{\partial^3 \phi_0}{\partial y^3} + \dots$$

The summations of ϕ_1 and ϕ_3 , and of ϕ_2 and ϕ_4 result in

$$\phi_1 + \phi_3 = \phi_{13} = 2\phi_0 + h_1^2 \frac{\partial^2 \phi_0}{\partial x^2} + O(h^4) \quad (\text{A.3})$$

and

$$\phi_2 + \phi_4 = \phi_{24} = 2\phi_0 + h_2^2 \frac{\partial^2 \phi_0}{\partial y^2} + o(h^4) \quad (\text{A.4})$$

Equations A.3 and A.4 can now be solved for $\partial^2 \phi_0 / \partial x^2$ and $\partial^2 \phi_0 / \partial y^2$ respectively to give

$$\frac{\partial^2 \phi_0}{\partial x^2} = \frac{1}{h_1^2} [\phi_{13} - 2\phi_0 - o(h^2)] \quad (\text{A.5})$$

and

$$\frac{\partial^2 \phi_0}{\partial y^2} = \frac{1}{h_2^2} [\phi_{24} - 2\phi_0 - o(h^2)] \quad (\text{A.6})$$

The addition of Eqs. A.5 and A.6 results in

$$\frac{\partial^2 \phi_0}{\partial x^2} + \frac{\partial^2 \phi_0}{\partial y^2} = \frac{1}{h_1^2} [\phi_{13} - 2\phi_0] + \frac{1}{h_2^2} [\phi_{24} - 2\phi_0] - o(h^2)$$

or

$$\nabla^2 \phi_0 = \frac{1}{h_1 h_2} \left[\frac{h_2}{h_1} (\phi_{13} - 2\phi_0) + \frac{h_1}{h_2} (\phi_{24} - 2\phi_0) \right] - o(h^2) \quad (\text{A.7})$$

Using $r = h_1/h_2$ Eq. A.7 can be rewritten as

$$\nabla^2 \phi_0 = \frac{1}{h_1 h_2} \left[\frac{1}{r} \phi_{13} + r \phi_{24} - 2 \left(\frac{1}{r} + r \right) \phi_0 \right] - o(h^2) \quad (\text{A.8})$$

From Eq. A.1 $\nabla^2 \phi = f(x, y)$ which means Eq. A.8 can be given as

$$f_0 = \frac{1}{h_1 h_2} \left[\frac{1}{r} \phi_{13} + r \phi_{24} - 2 \left(\frac{1}{r} + r \right) \phi_0 \right] - o(h^2) \quad (\text{A.9})$$

Then solving Eq. A.9 for ϕ_0 results in

$$\phi_0 = \frac{1}{2 \left(\frac{1}{r} + r \right)} \left[\frac{1}{r} \phi_{13} + r \phi_{24} - h_1 h_2 (f_0) \right] - o(h^2) \quad (\text{A.10})$$

Or using standard notation the five-point finite difference approximation for Poisson's equation can be written as

$$\begin{aligned} \phi_{i,j} = & \frac{1}{2(\frac{1}{r} + r)} \left[\frac{1}{r} (\phi_{i+1,j} + \phi_{i-1,j}) + r(\phi_{i,j+1} + \phi_{i,j-1}) \right. \\ & \left. - h_1 h_2 (f_{i,j}) \right] - O(h^2) \end{aligned} \quad (A.11)$$

APPENDIX B. FLOW CHART OF COMPUTER PROGRAM USED BY THIS STUDY

